DALTON
FULL PAPER

Non-planar porphyrins with mixed substituent pattern: bromination and formylation of ethyl-substituted tetraphenylporphyrins and tetraalkylporphyrins

Mathias O. Senge,*[a] Vanessa Gerstung,[a] Karin Ruhlandt-Senge,[b] Steffen Runge[a] and Ingo Lehmann[a]

[a] *Institut für Organische Chemie (WE02), Fachbereich Chemie, Freie Universität Berlin, Takustr. 3, D-14195 Berlin, Germany. E-Mail: mosenge@chemie.fu-berlin.de*
[b] *Department of Chemistry, Syracuse University, Syracuse, NY 13244, USA*

Received 17th August 1998, Accepted 27th October 1998

A series of 5,10,15,20-tetraphenylporphyrins (TPPs) bearing different numbers and orientations of β-ethyl substituents have been used for studies on the functionalization of non-planar porphyrins. Attempts to monofunctionalize the diethyl-TPP *via* monobromination failed and resulted in the isolation of two different regioisomers. All ethyl-TPPs were easily converted into the perbrominated porphyrins bearing twelve peripheral substituents but with different numbers of β-bromo and -ethyl groups. These porphyrins are interesting precursors for further mixing of the substituent pattern and are novel push-pull porphyrins bearing electron donating and withdrawing groups in a defined pattern directly on the ring system. They have a similar degree of overall conformational distortion, however each with considerably altered electronic effects due to the different number of bromine atoms. In order to gain access to monofunctionalized derivatives, some of the ethyl-TPPs were converted into the monoformyl derivatives. In a similar manner, a number of 5,10,15,20-tetraalkylporphyrins were formylated, albeit in lower yields than the ethyl-TPPs. Several compounds were investigated in detail by single crystal X-ray crystallography and allowed a comparison of the influence of different substituent patterns on the conformation. The structural analyses include a comparison of different crystalline modifications for some compounds. Structural data for perbrominated ethyl-TPPs present the first examples of highly non-planar, dodecasubstituted porphyrins bearing two different types of β-substituents.

Introduction

Non-planar porphyrins have attracted much interest in the last decade and are used to mimic the conformationally distorted porphyrins found *in vivo*.[1] Synthetic non-planar porphyrins are utilized to model the effects of the protein backbone on the chromophore properties in intact pigment–protein complexes. Prime candidates for such investigations have been the so-called "highly substituted porphyrins", where the introduction of sterically demanding substituents at the porphyrin periphery leads to significantly non-planar macrocycle conformations.[2] Most highly substituted porphyrins currently utilized in model studies fall into the class of symmetric, dodecasubstituted porphyrins. Two prime examples for these are the 2,3,7,8,12,13,17,18-octaalkyl-5,10,15,20-tetraarylporphyrins[3] and the 2,3,7,8,12,13,17,18-octahalogeno-5,10,15,20-tetraarylporphyrins.[4–7] The latter porphyrins have considerable potential as technically applicable catalysts.[8] Most of these dodecasubstituted porphyrins exhibit saddle-shaped distortions with maximum displacements of the C_b positions in the range of 1–1.2 Å [C_m = *meso* carbon atoms 5,10,15,20; C_b = β-pyrrole positions 2,3,7,8,12,13,17,18].

These symmetric porphyrins are easily obtained by tetramerization of 3,4-disubstituted pyrroles and aldehyde[9] or, in the case of β-halogenoporphyrins, *via* halogenation of 5,10,15,20-tetraarylporphyrins.[10] To our knowledge, no asymmetric dodecasubstituted porphyrins have been described that carry more than one type of β substituent. In addition, no reports have been made on the subsequent monofunctionalization of such dodecasubstituted porphyrins, the exception being the Suzuki cross-coupling of octabromotetraarylporphyrins.[11] Nevertheless, functionalized non-planar porphyrins are necessary to provide a convenient entry into multicomponent porphyrin systems or for the preparation of donor–acceptor compounds with specifically designed conformational distortion.[12] Such systems would then allow studying the effects of various distortion modes on the physicochemical properties in more complex systems than those presently utilized. Detailed physicochemical studies would preferably require a series of functionalized porphyrins with graded degrees of conformational distortion. We have recently described a series of porphyrins with graded degrees of saddle distortion ML^1–ML^6.[13] The porphyrins ML^2–ML^5 have free β positions amenable for further transformations and we describe here our results on the bromination and formylation of these compounds in conjunction with structural studies on some of the target compounds.

Results and discussion

Initially we were interested in obtaining access to porphyrins with one functionality for further coupling reactions, *e.g.* monobromo and monoformyl porphyrins. Thus, we investigated the possibility to monobrominate L^2. Several different procedures have been described to β-brominate porphyrins.[11,14,15] We first tested the method developed by Callot for the mono- and poly-bromination of tetraphenylporphyrin H_2L^1.[15] Treatment of H_2L^2 with 2 equivalents *N*-bromosuccinimide (NBS) in chloroform gave a complex mixture of products. Despite repeated purification attempts, including the use of HPLC, only one compound could be isolated in pure form and in very low yield. The product was identified as the symmetric 2,13-dibromo-7,8-diethyl-5,10,15,20-tetraphenylporphyrin H_2L^9, while the remainder of the material constituted various regioisomers of polyhalogenated porphyrins. A similar result was obtained, when exactly 1 equivalent NBS was used and the reaction was stopped after TLC showed the beginning

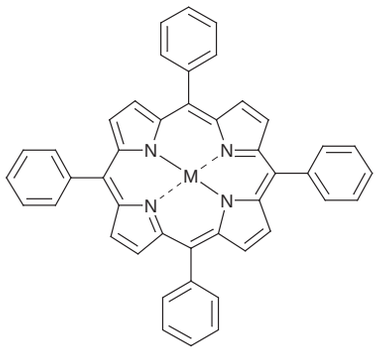

ML^1

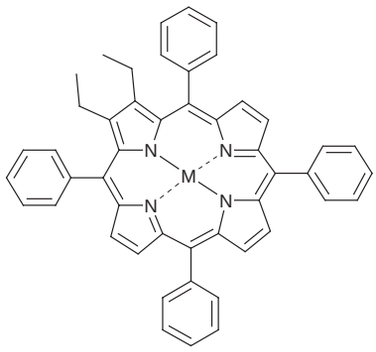

ML^2

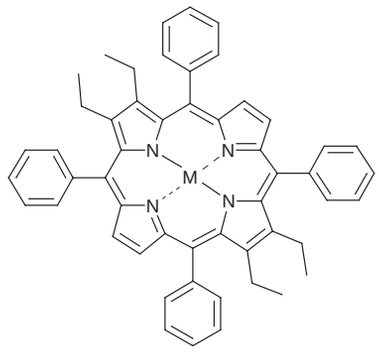

ML^3

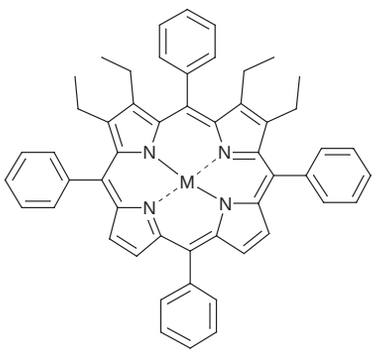

ML^4

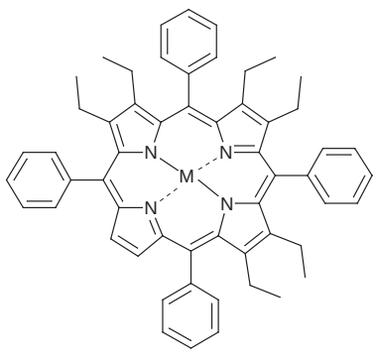

ML^5

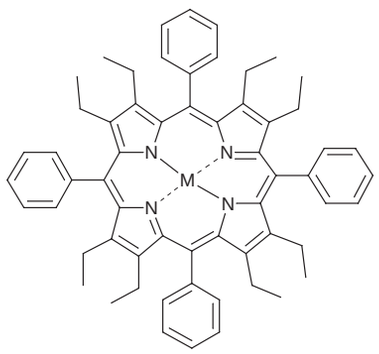

ML^6

of product formation. Nevertheless, a complex mixture was obtained from which only the asymmetrically substituted 2,12-dibromo-7,8-diethyl-5,10,15,20-tetraphenylporphyrin H_2L^{10} could be isolated in low yields. Further modifications of the reaction conditions gave similar results.

In fact, monobromination does occur but all attempts to separate compound H_2L^8 from the dibrominated derivatives H_2L^9 or H_2L^{10} failed. Conclusive proof for monobromination was obtained from single crystals separated manually from other crystals of the reaction mixture, that led to the formation of H_2L^{10}. One such crystal was investigated by X-ray crystallography and NMR and was shown to consist of a mixture of 2-bromo-7,8-diethyl-5,10,15,20-tetraphenylporphyrin (H_2L^8, *ca*. 90%) and H_2L^{10} (*ca*. 10%) (not shown).

Despite the discouraging synthetic results, the two regioisomers H_2L^9 and H_2L^{10} presented a unique chance to study the effects of the different substituent pattern on the macrocycle conformation. While several crystal structures of β-bromoporphyrins have been published, these are either 2,3,12,13-tetrabromo-5,10,15,20-tetraarylporphyrins[16] or octabromotetraarylporphyrins,[4–7] *i.e*. carrying either four or eight β-bromo substituents. Single crystals suitable for X-ray analysis could be grown quite easily for both H_2L^9 and H_2L^{10}. Interestingly, compound H_2L^9 crystallized in both an orthorhombic (not shown) and monoclinic modification (Fig. 1) without inclusion of solvent molecules. The regioisomers H_2L^9 and H_2L^{10} (Fig. 2) have different sets of potentially sterically hindered areas. Compound L^{10} has one pattern of (Br,Ph,H), (H,Ph,H), (Et,Ph,H) and (Et,Ph,Br) substituents while L^9 has two patterns of (Br,Ph,H) and (Et,Ph,H) substituents. Thus, L^{10} has one *meso*-phenyl group (C10) flanked by two non-hydrogen substituents (Br, Et) while L^9 carries only phenyl groups flanked with one non-hydrogen substituent (either Et or Br). As a result a more non-planar conformation was expected for H_2L^{10}.

This expectation is confirmed by a simple visual inspection of the skeletal deviations of the three porphyrins (Fig. 3). A more detailed analysis shows that the mean deviation of the 24 macrocycle atoms from their least-squares plane (Δ24) decreases in the order H_2L^{10} > H_2L^9, monoclinic > H_2L^9 orthorhombic, with Δ24 = 0.38, 0.22 and 0.16 Å, respectively (Table 1). All three structures exhibit a saddle conformation (large deviations from planarity for the C_b positions) with some degree of ruffling distortion (significant deviations from planarity for the C_m positions) mixed in (for definition of the

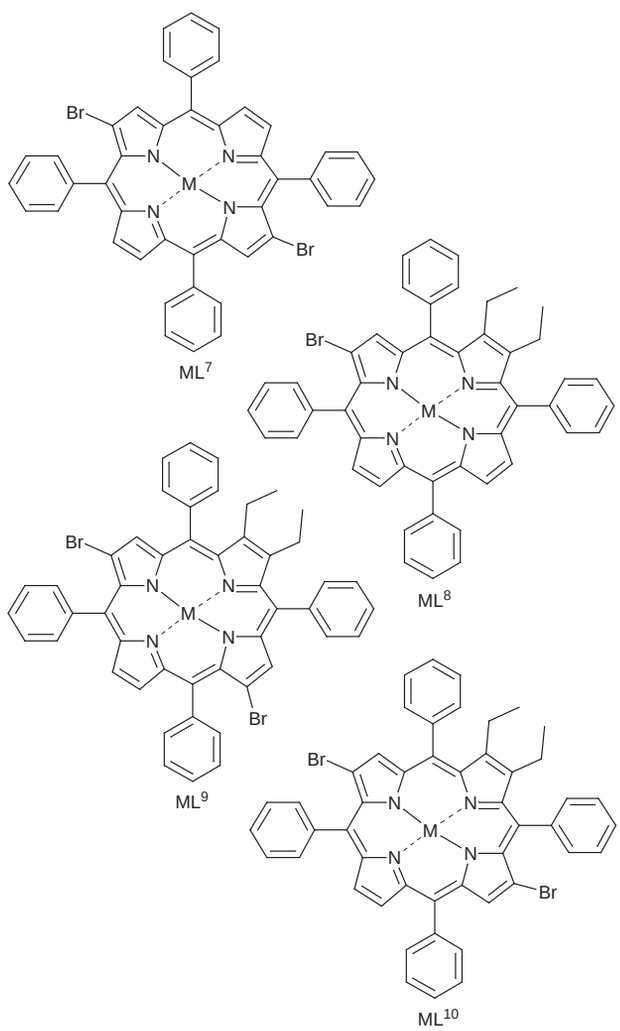

ML^7

ML^8

ML^9

ML^{10}

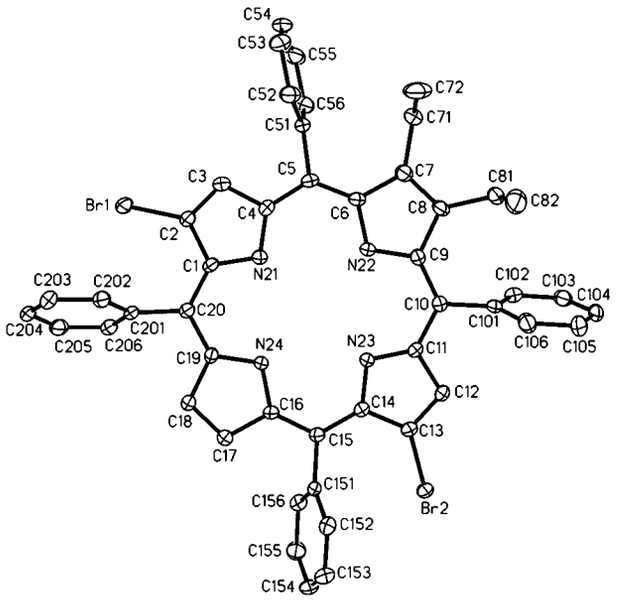

Fig. 1 Computer generated plot of the molecular structure of the monoclinic modification of H_2L^9 in the crystal. Hydrogen atoms have been omitted for clarity and thermal ellipsoids are drawn for 50% occupancy.

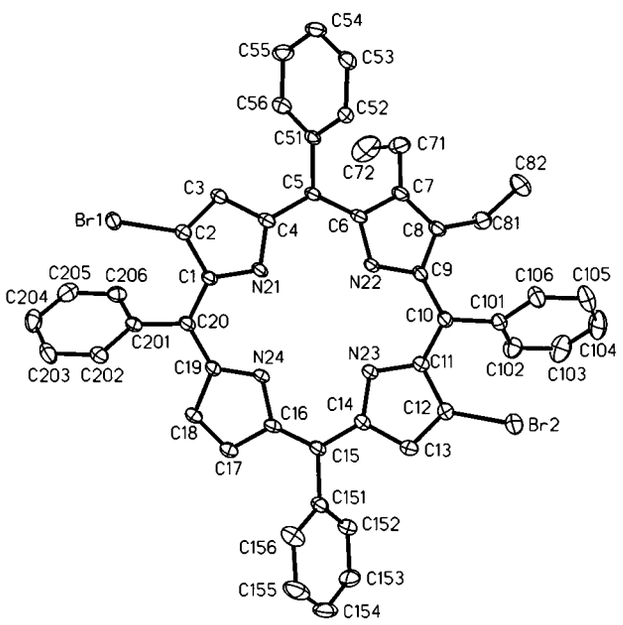

Fig. 2 Computer generated plot of the molecular structure of H_2L^{10} in the crystal. Details as in Fig. 1.

various distortion modes see refs. 17 and 18). In line with the expectation that lowering the symmetry of the porphyrin leads to mixing of different distortion modes,[19,20] the degree of ruffling is much larger in the asymmetric H_2L^{10} (significantly larger C_m displacements). General structural trends are in agreement with those now well established for symmetric non-planar porphyrins (Table 2).[3–7,17] In agreement with the asymmetric substituent pattern the core conformation is not symmetric. Notably, H_2L^{10} shows a significant degree of in-plane distortion. This is evidenced by the core elongation parameter, the difference between the pairs of neighboring N–N vector lengths. The core is elongated by 0.128 Å along the N21–N22 axis while no such elongation is observed in both structures of H_2L^9 or for that matter in any other structure described herein.

The overall degree of conformational distortion in the two modifications of H_2L^9 is similar. The main difference between the two modifications is the relative orientation of the C7- and

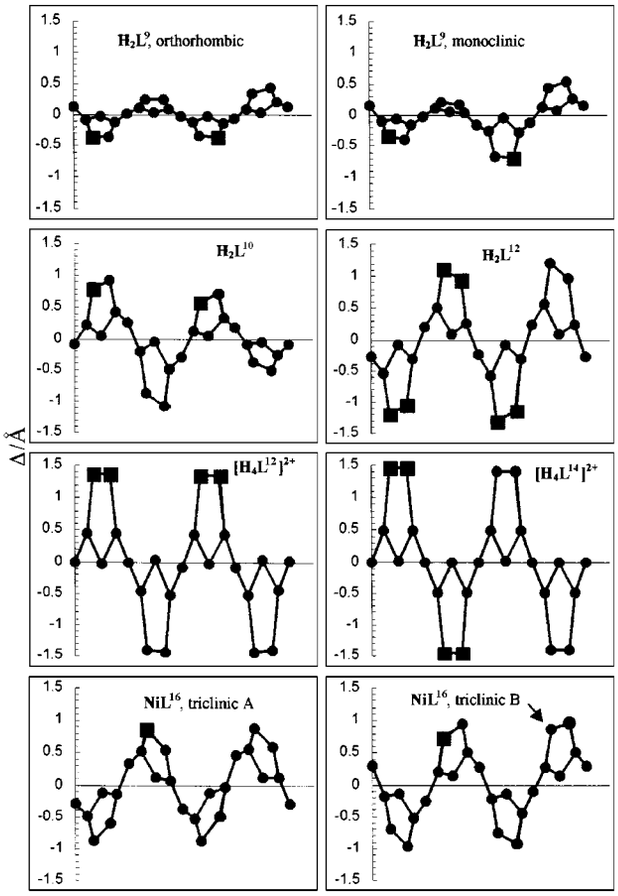

Fig. 3 Linear display of the skeletal deviations of the macrocycle atoms from the 4N plane for selected porphyrins. The *x* axis is not to scale. The symbol ■ denotes positions of β bromination or formylation in the respective porphyrins. The arrow in the display of NiL^{16} (triclinic B) indicates the minor formyl position.

C8-ethyl groups and the degree of displacement found for pyrrole ring III which is significantly larger in the monoclinic modification, a further indication for the inherent conformation flexibility of highly substituted porphyrins.[21] The steric influence of the individual substituents can clearly be delineated in each macrocycle. For example in H_2L^{10}, the largest deviations are found for pyrrole rings with two ethyl groups, with smaller deviations for the monobrominated and unsubstituted pyrrole rings. In H_2L^9 the situation is reversed with the largest displacements found for the C_b positions of the brominated pyrrole rings. Analysis of the crystal packing gave no significant evidence that close contacts were responsible for the differences in conformation. For both modifications of H_2L^9 the closest non-hydrogen interactions were found between Br1 and Br2, that were separated by 3.486 Å in the monoclinic and 3.529 Å in the orthorhombic modification. Compound H_2L^{10} exhibited a very weak interaction between a β-hydrogen (H3) and Br1 (2.91 Å). In all three structures the pyrrole hydrogen atoms were found to be located at the pyrrole nitrogen atoms involving the unbrominated rings.

As expected, these three structures are much less non-planar than dodecasubstituted porphyrins like H_2L^6. Nevertheless, individual displacements like those found for the diethylpyrrole unit in H_2L^{10} come close to those observed for dodecasubstituted non-planar porphyrins. A direct comparison of the structural data with other porphyrins is not possible. While a number of tetra-β-substituted *meso*-arylporphyrin structures have been reported, those containing bromo-substituents belong to the 2,3,12,13-tetrabromo-5,10,15,20-tetraarylporphyrin class.[16] Other examples are the various structures of H_2L^3 and H_2L^4 reported by us [13b] and related com-

Table 1 Selected conformational parameters for the porphyrins studied (deviations in Å, angles in °)

Compound	H_2L^9		H_2L^{10}	H_2L^{12} tricl. B	$[H_4L^{12}]^{2+}$	$[H_4L^{14}]^{2+}$	NiL^{16}	
	Orthogonal	Monoclinic					Triclinic	Monoclinic
$\Delta 24^a$	0.164	0.22	0.38	0.56	0.63	0.64	0.425	0.47
$\otimes^b$	2.081	2.076	2.063	2.042	2.14	2.101	1.920	1.926
Ξ^c	−0.04	−0.003	0.128	0.031	0	0.027	−0.008	0.015
φ_{pyr} N21 ^{d}	8.9	8.6	22.4	29.4	43.6	44.7	19.1	21.2
φ_{pyr} N22	5.9	4.1	27.2	28.0	41.4	40.8	20.2	30.6
φ_{pyr} N23	8.5	16.3	17.1	32.8	*e*	*e*	20.6	20.2
φ_{pyr} N24	10.3	12.7	11.8	30.3	40.4	*e*	20.5	21.7
φ_{ar} C5 ^{f}	80.8	86.3	41.9	40.6	23.6	14.9	59.6	51.0
φ_{ar} C10	77.2	72.8	55.6	48.0	*e*	18.3	67.0	52.1
φ_{ar} C15	84.6	65.4	57.2	36.6	*e*	32.9	55.9	52.0
φ_{ar} C20	62.9	71.3	46.9	48.4	23.0	*e*	63.8	57.7
$>_{ar/Cm}$ C5 ^{g}	86.1	87.4	55.3	59.9	44.9	37.6	73.5	70.1
$>_{ar/Cm}$ C10	82.0	79.4	69.0	67.2	*e*	41.9	81.0	69.6
$>_{ar/Cm}$ C15	89.7	74.8	67.0	58.2	*e*	55.8	69.6	69.7
$>_{ar/Cm}$ C20	69.6	79.6	58.2	66.0	45.2	*e*	79.1	72.2
δC_m C5 ^{h}	0.01	0.02	0.25	0.21	0.01	0	0.34	0.26
δC_m C10	0.03	0.17	0.30	0.24	*e*	0	0.38	0.28
δC_m C15	0.06	0.13	0.19	0.23	*e*	0	0.47	0.1
δC_m C20	0.13	0.15	0.09	0.28	0.09	*e*	0.29	0.30
δC_b N21 ^{c}	0.35	0.36	0.86	1.12	1.43	1.46	0.74	0.83
δC_b N22	0.24	0.18	0.97	1.06	1.36	1.40	0.70	0.84
δC_b N23	0.34	0.68	0.65	1.22	*e*	*e*	0.67	0.84
δC_b N24	0.38	0.49	0.44	1.09	1.34	*e*	0.75	0.92

^{a} Deviation of the 24 macrocycle atoms from their least squares plane. ^{b} Core size defined as the geometrical center of the four nitrogen atoms. ^{c} Core elongation parameter defined as the difference between the vector lengths (|N21–N22|+|N23–N24|) − (|N22–N23|+|N21–N24|). ^{d} Pyrrole tilt angle with the 4N plane. ^{e} Generated by symmetry operations. ^{f} Phenyl tilt angle against the 4N plane. ^{g} Phenyl tilt against the C_a–C_m–C_a plane. ^{h} Deviation of the C_m carbon atoms from the 4N plane. ^{i} Average deviation of the C_b atoms from the 4N plane.

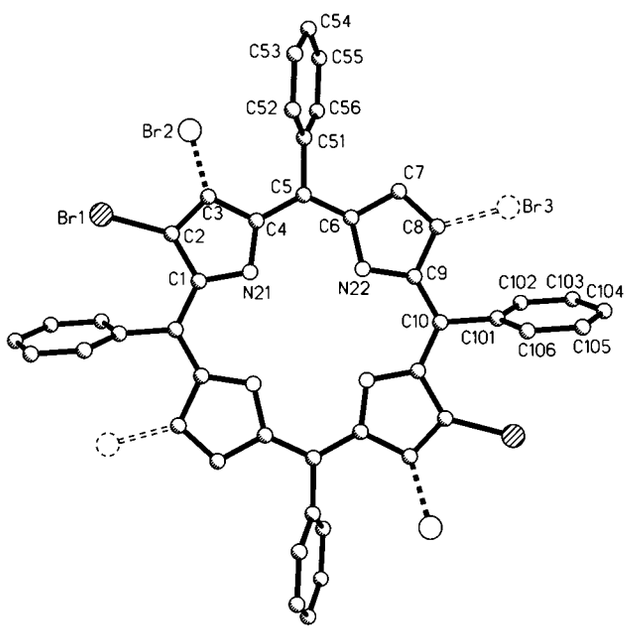

Fig. 4 Computer generated plot of the molecular structure of H_2L^7 in the crystal. Hydrogen atoms have been omitted for clarity. All three sets of rotationally disordered bromo substituents are shown (minor components with dashed lines).

pounds.[11a,22] In line with expectations[1a] H_2L^{10} shows a small bathochromic shift of the absorption maxima compared to H_2L^9 indicating a more non-planar conformation in solution.

For comparative purposes we prepared the dibromoporphyrin H_2L^7 according to the method given by Giraudeau *et al.*[23] Unfortunately, crystallographic analysis showed this compound to be a prime example for rotational disorder in the crystal. As shown in Fig. 4, three different sets of 2,12-dibromo substituents are present in the crystal preventing detailed conformational analysis. Overall, the macrocycle shows only moderate distortion with a Δ24 of 0.06 Å, *i.e.* H_2L^7 is significantly more planar than the respective diethyl derivatives H_2L^9 or H_2L^{10}. The largest individual displacements are observed for C7 and C8 which show displacements from the 4N plane in the order of 0.42 Å. Significant ruffling is present as indicated by C_m displacements of 0.19 Å for C5 and 0.16 Å for C10, respectively. The core size in H_2L^7 was determined to be 2.089 Å. The only compound with a similar substituent arrangement is 7,18-dinitro-5,10,15,20-tetraphenylporphyrin, that also shows a saddle deformation.[24]

We next turned our attention to the preparation of porphyrins in which all the free β positions of the porphyrins H_2L^2–H_2L^5 would be substituted with bromine atoms. Such porphyrins should have a very similar overall degree of conformational distortion albeit with quite different redox potentials depending on the number of bromine atoms and present the first examples of "push-pull porphyrins" where +I and −I groups are located directly at the porphyrin ring system In addition, such porphyrins present excellent precursors for other dodeca-substituted porphyrins with mixed substituent pattern *via* Suzuki coupling.[11] Perbromination of tetraarylporphyrins has been widely used and is generally achieved quite easily when the respective metalloporphyrins are used for bromination.[10]

For the preparation of the porphyrins H_2L^{12}–H_2L^{15} we used a method similar to that described by Bhyrappa and Krishnan,[10a] however using nickel(II) or zinc(II) porphyrins as starting material. The perbromination proceeded smoothly and gave the target compounds in about 50% yield. In all cases, standard work-up resulted in the isolation of the respective perbrominated free-base porphyrins. Subsequently, we transformed the free base porphyrins into the respective nickel(II) complexes NiL^{12}–NiL^{15} and prepared ZnL^{12} by standard procedures.

A comparison of the spectroscopic data for the free base porphyrins and the nickel(II) complexes showed overall very similar characteristics with a slight tendency towards more red-shifted absorption maxima with increasing number of bromine atoms. For example, the long wavelength absorption bands in dichloromethane for the free base porphyrins H_2L^{11}–H_2L^{15} are 743, 732, 722, 726 and 711 nm, respectively. For comparison, the related value for H_2L^6 is 706 nm. Under the assumption that a bromine substituent is as sterically demanding as an alkyl

Table 2 Selected bond lengths (Å) and angles (°) for the macrocycle atoms of the dibromoporphyrins H_2L^9 and H_2L^{10}

	H_2L^9		
	Orthorhombic	Monoclinic	H_2L^{10}
N(21)–C(4)	1.371(3)	1.364(4)	1.379(3)
N(21)–C(1)	1.386(3)	1.371(3)	1.372(3)
N(22)–C(9)	1.383(3)	1.379(3)	1.381(3)
N(22)–C(6)	1.387(3)	1.387(3)	1.376(3)
N(23)–C(11)	1.373(3)	1.359(3)	1.376(3)
N(23)–C(14)	1.384(3)	1.388(3)	1.368(3)
N(24)–C(16)	1.376(3)	1.370(3)	1.383(3)
N(24)–C(19)	1.387(3)	1.372(3)	1.375(3)
C(1)–C(20)	1.409(3)	1.406(4)	1.424(3)
C(1)–C(2)	1.472(3)	1.470(4)	1.467(3)
C(2)–C(3)	1.341(3)	1.344(4)	1.360(3)
C(3)–C(4)	1.456(3)	1.459(4)	1.447(3)
C(4)–C(5)	1.421(3)	1.418(4)	1.418(3)
C(5)–C(6)	1.404(3)	1.398(4)	1.418(3)
C(6)–C(7)	1.453(3)	1.451(4)	1.442(3)
C(7)–C(8)	1.375(3)	1.374(4)	1.389(4)
C(8)–C(9)	1.454(3)	1.460(4)	1.450(3)
C(9)–C(10)	1.408(3)	1.403(4)	1.409(4)
C(10)–C(11)	1.422(3)	1.423(4)	1.420(3)
C(11)–C(12)	1.456(3)	1.460(4)	1.467(4)
C(12)–C(13)	1.349(3)	1.346(4)	1.361(4)
C(13)–C(14)	1.476(3)	1.464(4)	1.448(4)
C(14)–C(15)	1.404(3)	1.402(4)	1.418(3)
C(15)–C(16)	1.409(3)	1.410(4)	1.390(3)
C(16)–C(17)	1.437(3)	1.427(4)	1.436(3)
C(17)–C(18)	1.368(3)	1.371(4)	1.361(4)
C(18)–C(19)	1.426(3)	1.427(4)	1.442(3)
C(19)–C(20)	1.406(3)	1.408(4)	1.401(4)
C(4)–N(21)–C(1)	105.65(16)	106.4(2)	106.0(2)
C(9)–N(22)–C(6)	111.26(17)	111.1(2)	111.2(2)
C(11)–N(23)–C(14)	105.92(17)	105.7(2)	105.9(2)
C(16)–N(24)–C(19)	110.28(17)	110.1(2)	110.5(2)
N(21)–C(1)–C(20)	124.77(18)	124.3(2)	123.8(2)
N(21)–C(1)–C(2)	109.09(17)	109.2(2)	109.5(2)
C(20)–C(1)–C(2)	126.05(18)	126.3(2)	126.7(2)
C(3)–C(2)–C(1)	107.56(18)	107.3(2)	107.3(2)
C(2)–C(3)–C(4)	106.43(19)	106.2(2)	106.1(2)
N(21)–C(4)–C(5)	127.38(19)	127.7(3)	125.3(2)
N(21)–C(4)–C(3)	111.08(17)	110.7(2)	111.0(2)
C(5)–C(4)–C(3)	121.49(19)	121.5(3)	123.6(2)
C(6)–C(5)–C(4)	126.32(19)	127.2(3)	125.2(2)
C(6)–C(5)–C(51)	120.25(18)	119.6(2)	118.0(2)
C(4)–C(5)–C(51)	113.36(18)	113.3(2)	116.8(2)
N(22)–C(6)–C(5)	124.01(18)	123.5(2)	125.2(2)
N(22)–C(6)–C(7)	106.07(18)	106.3(2)	106.4(2)
C(5)–C(6)–C(7)	129.9(2)	130.0(3)	128.4(2)
C(8)–C(7)–C(6)	108.24(19)	108.3(2)	108.3(2)
C(7)–C(8)–C(9)	108.34(18)	108.0(2)	107.4(2)
N(22)–C(9)–C(10)	124.62(18)	124.1(2)	122.9(2)
N(22)–C(9)–C(8)	106.08(18)	106.3(2)	106.4(2)
C(10)–C(9)–C(8)	129.25(18)	129.5(2)	130.6(2)
C(9)–C(10)–C(11)	127.06(18)	127.1(2)	123.7(2)
N(23)–C(11)–C(10)	127.93(19)	127.6(2)	124.2(2)
N(23)–C(11)–C(12)	111.14(18)	111.5(2)	109.1(2)
C(10)–C(11)–C(12)	120.92(19)	120.9(2)	126.5(2)
C(13)–C(12)–C(11)	106.38(18)	106.0(2)	107.6(2)
C(12)–C(13)–C(14)	107.41(18)	107.5(2)	105.4(2)
N(23)–C(14)–C(15)	124.44(18)	123.8(2)	125.4(2)
N(23)–C(14)–C(13)	109.14(17)	109.4(2)	111.7(2)
C(15)–C(14)–C(13)	126.42(19)	126.8(2)	122.7(2)
C(14)–C(15)–C(16)	124.22(19)	124.5(2)	125.3(2)
N(24)–C(16)–C(15)	127.6(2)	127.0(2)	126.3(2)
N(24)–C(16)–C(17)	106.64(18)	107.0(2)	106.4(2)
C(15)–C(16)–C(17)	125.7(2)	125.9(2)	127.3(2)
C(18)–C(17)–C(16)	108.0(2)	107.9(2)	108.5(2)
C(17)–C(18)–C(19)	108.56(19)	107.9(2)	108.2(2)
N(24)–C(19)–C(20)	126.36(19)	126.8(2)	125.8(2)
N(24)–C(19)–C(18)	106.48(17)	106.9(2)	106.4(2)
C(20)–C(19)–C(18)	127.13(19)	126.1(2)	127.5(2)
C(19)–C(20)–C(1)	124.83(18)	124.4(2)	123.2(2)

residue and that all these porphyrins have similar conformations, this clearly reveals an additional electronic effect of the bromine atoms on the absorption spectra. For a more theoretical discussion of this effect see ref. 10(*a*).

Structural analyses of the perbrominated porphyrins proved to be challenging. In line with the expectation that a bromine substituent induces the same conformational distortion as a β-alkyl group, the overall conformations of the β-brominated porphyrins are roughly similar to each other and to that of 2,3,7,8,12,13,17,18-octaalkyl-5,10,15,20-tetraarylporphyrins. This led to disorder involving β-ethyl and -bromo groups in the crystal. In most cases these effects prevented a satisfactory refinement of the structural data.

First, we crystallized H_2L^{12} from $CHCl_3$–cyclohexane and obtained crystals of a triclinic cyclohexane solvate (triclinic A modification). The structure (not shown) could not be refined satisfactorily due to disorder of the bromine and ethyl substituents. Thus, only overall structural parameters will be given here. The conformation is that of a severely distorted saddle (Δ24 = 0.55 Å) with a slight degree of ruffling. The pyrrole tilt angles against the 4N plane are 34, 36, 25 and 29° for N21, N22, N23, and N24, respectively (e.s.d.s *ca*. 1°). The maximum displacements of a C_m atom are 0.12 Å for C10; the C_b displacements were found to be 0.93–1.27 Å (e.s.d.s *ca*. 0.05 Å).

A second triclinic modification of H_2L^{12} crystallized with two dichloromethane molecules of solvation (triclinic B modification). In this modification two independent molecules were present, one of which showed no disorder. The refinement proceeded more straightforwardly than for the triclinic A modification. Thus, only data of the non-disordered molecule 1 of the triclinic B modification are used for further structural discussions (Fig. 5). The molecular structure exhibits a severely saddle-distorted macrocycle with a Δ24 of 0.56 Å and average C_b displacements ranging from 1.06 to 1.22 Å. Again, a significant degree of ruffling is present in the structure with C_m displacements of the order of 0.24 Å. The disordered second independent molecule in the asymmetric unit showed a similar conformation and degree of distortion (Δ24 = 0.546 Å).

Thus, the overall degree of distortion is indeed similar to that of octa-β-alkyltetraarylporphyrins like H_2L^6 which shows a Δ24 of 0.54 A and average C_b displacements of 1.17 Å. Note, that even in the symmetric H_2L^6 the C_b displacements of individual pyrrole rings vary between 1.03 and 1.27 Å.[3b] Two crystalline modifications of H_2L^{11} have been described.[5,6] Both exhibit conformations similar to that of H_2L^{12}. For example, the average C_b displacement in the DMF solvate of H_2L^{11} is 1.26 Å while the average C_m displacement is 0.32 Å.[5] Thus, the main structural difference between compounds like H_2L^6 and the β-bromoporphyrins is the significantly larger C_m displacement in the latter.

Since none of the metalloporphyrins H_2L^{12}–H_2L^{15} produced satisfactory crystal quality we attempted crystallization of the respective porphyrin dications in the form of their trifluoroacetate salts. Two such samples gave crystals suitable for X-ray analysis. The $[H_4L^{12}]^{2+}$ dication exhibits an almost pure saddle distortion with a Δ24 of 0.63 Å and an average C_b displacement of 1.37 Å (Figs. 6 and 3). Thus, the dication is considerably more non-planar than the respective free base H_2L^{12}. This is in full agreement with our earlier investigation on the $[H_4L^{11}]^{2+}$ dication (Δ24 = 0.69 Å, δC_b = 1.52 Å).[7] The dication of the octabromo derivative H_2L^{11} shows significantly larger C_b displacements than that of the hexabromodiethyl derivative H_2L^{12}. In fact, the conformation of the ditriflate of $[H_4L^{12}]^{2+}$ is quite similar to that of $[H_4L^6]^{2+}$ (Δ24 = 0.63 Å, δC_b = 1.38 Å).[25] One interesting difference to other structures of trifluoroacetate salts of dodecasubstituted dications is the observation of mono- and bi-dentate binding of the TFA units to the porphyrin core. Other structures exhibited only bidentate binding.[7,25] Note that the TFA bound in monodentate fashion is present in the crystal in two different orientations. The relevant

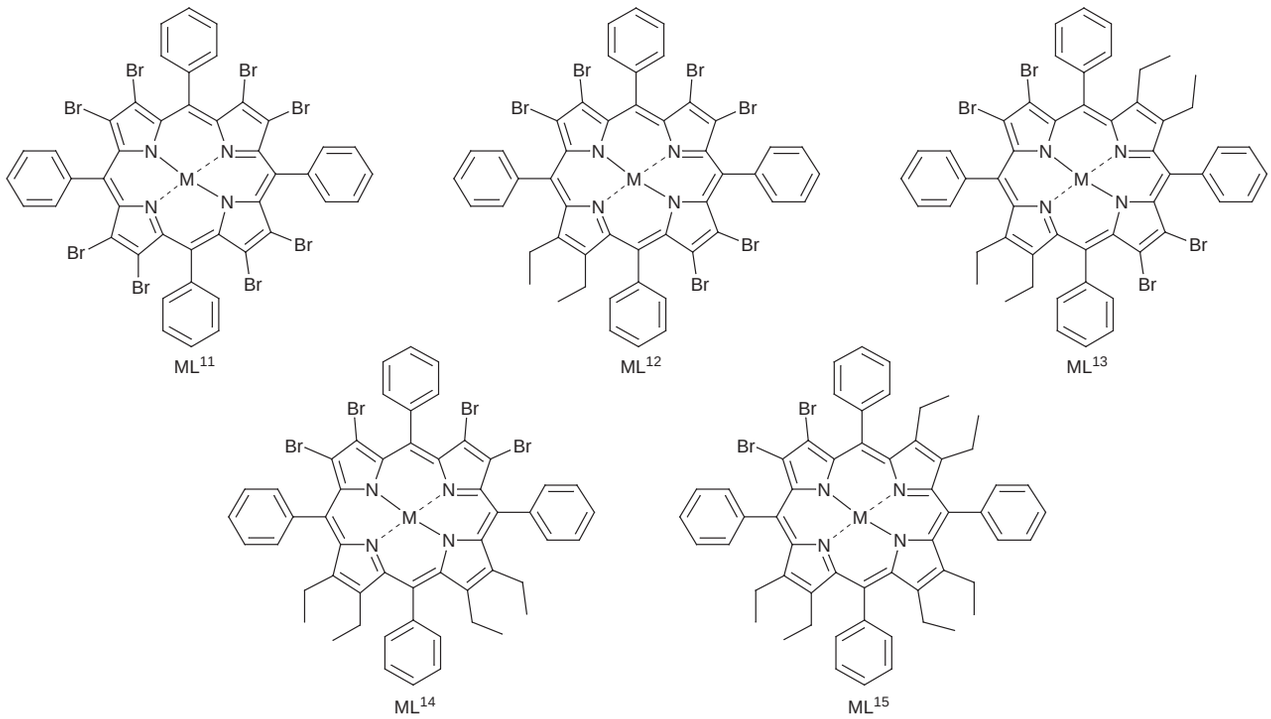

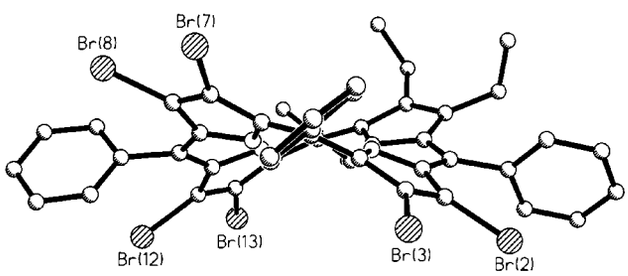

Fig. 5 Computer generated side view of the molecular structure of the triclinic B modification of H_2L^{12} in the crystal. Hydrogen atoms have been omitted for clarity.

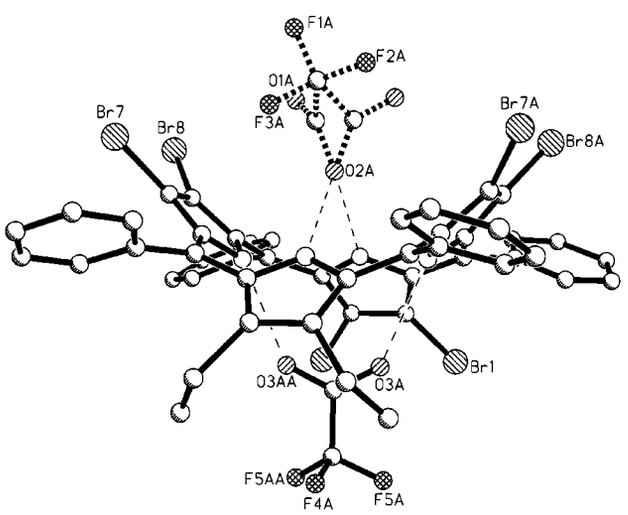

Fig. 6 Computer generated side view of the molecular structure of $[H_4L^{12}][CF_3CO_2]_2$ in the crystal. Hydrogen atoms have been omitted for clarity and both orientations are shown for the disordered hydrogen bonded trifluoroacetate. Weak dashed lines indicate hydrogen bonds.

hydrogen bond distances in $[H_4L^{12}]^{2+}$ are: N22···O3A 2.646, H22···O3A 1.876, N21···O2A 2.863, H21···O2A 1.991, N23···O2A 2.820 and H23···O2A 1.946 Å.

The conformation of the triflate salt of $[H_4L^{14}]^{2+}$ is quite similar to that of $[H_4L^{12}]^{2+}$ the distortion being characterized by a Δ24 of 0.64 Å and an average C_b displacement of 1.43 Å

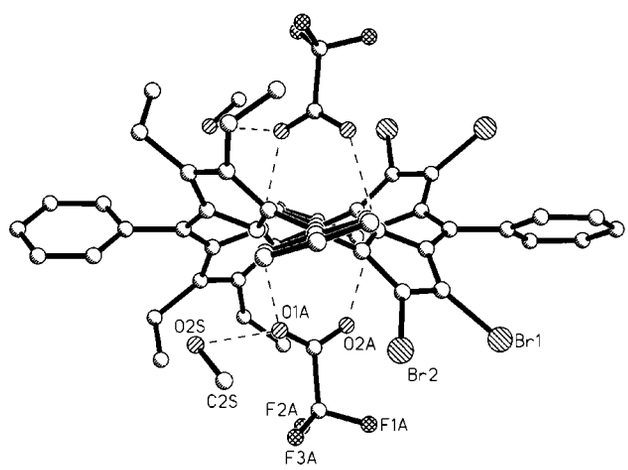

Fig. 7 Computer generated side view of the molecular structure of $[H_4L^{14}][CF_3CO_2]_2$ in the crystal. Hydrogen atoms have been omitted for clarity. Weak dashed lines indicate hydrogen bonds.

(Fig. 7). As observed for $[H_4L^{12}]^{2+}$ the distortion mode is quite symmetric (Fig. 3) and shows only small differences between β-bromo and β-ethyl quadrants. In this case both TFA molecules are hydrogen bonded in a bidentate fashion to the hydrogen atoms of the porphyrin core. The relevant hydrogen bond distances in $[H_4L^{12}]^{2+}$ are: N21···O2A 2.730, H21···O2A 1.998, N22···O1A 2.691 and H22···O1A 2.032 Å. One of the TFA anions is hydrogen bonded to a methanol of solvation (O1A···O2S 2.787 Å). In both dication structures a number of aryl hydrogen halogen contacts in the range of 3 Å were observed. The closest non-hydrogen contacts were bromo–bromo or bromo–solvent contacts in the range of 3.6–3.7 Å.

In order to gain access to other asymmetrically, highly substituted porphyrins and to obtain the desired monofunctionalized porphyrins described above we performed Vilsmeier formylations[26] on the porphyrins NiL^2–NiL^5. Obviously, formylation of NiL^2 and NiL^4 gives a regioisomeric mixture (e.g. NiL^{17}/NiL^{18}) and thus was performed only for test purposes. While it is possible to separate the different regioisomers by HPLC it was found to be not feasible. The formylation of both NiL^3 and NiL^5 proceeded smoothly with acceptable yields and the spectroscopic data indicated that introduction of β-formyl

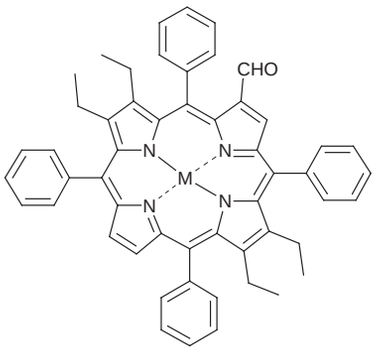

ML[16]

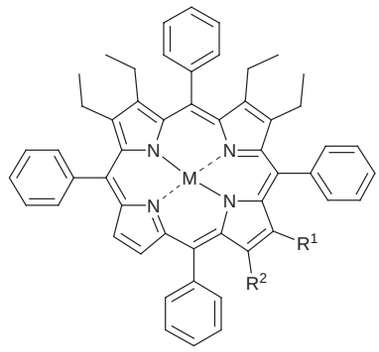

ML[17] R^1 = CHO, R^2 = H
ML[18] R^1 = H, R^2 = CHO

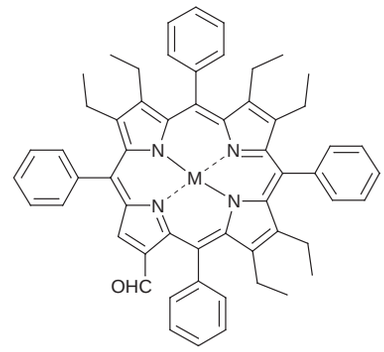

ML[19]

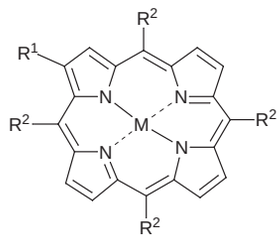

ML[20] R^1 = H, R^2 = nBu
ML[21] R^1 = H, R^2 = $CH_2CH(CH_3)_2$
ML[22] R^1 = H, R^2 = iPr
ML[23] R^1 = H, R^2 = $CH(CH_2CH_3)_2$
ML[24] R^1 = H, R^2 = tBu
ML[25] R^1 = CHO, R^2 = nBu
ML[26] R^1 = CHO, R^2 = $CH_2CH(CH_3)_2$
ML[27] R^1 = CHO, R^2 = iPr
ML[28] R^1 = CHO, R^2 = $CH(CH_2CH_3)_2$

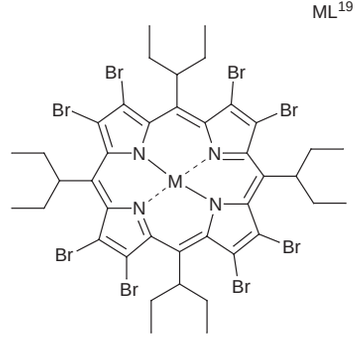

ML[29]

groups leads to a small but detectable bathochromic shift (about 6 nm).

For compound NiL[16] two crystal structure determinations were performed. A triclinic modification (not shown) contained chloroform and water solvate molecules while the monoclinic modification was identified as a dichloromethane solvate (Fig. 8). In the latter case the dichloromethane is located in the "binding pocket" formed by the β-ethyl "arms" (separation between Ni and C1S = 3.599 Å), a situation frequently encountered in non-planar porphyrins. The molecule forms dimer type structures in the crystal in which one face of the porphyrin is blocked by the dichloromethane molecule and the other side shows a Ni–H55 (an *o*-phenyl hydrogen) contact of 2.974 Å. Both modifications show a highly non-planar conformation characterized by a mixing of saddle and ruffle distortion modes. The degree of ruffling is much larger in the triclinic modification (δC_m = 0.29–0.47, δC_b = 0.67–0.75 Å) than in the monoclinic modification (δC_m = 0.1–0.30, δC_b = 0.83–0.92 Å). This provides evidence for considerable flexibility in the degree of mixing of different distortion modes possible in asymmetrically substituted porphyrins. A direct comparison was not possible with the structure of the starting material NiL[3], which so far has been identified only in a highly ruffled conformation. All other ethyl-TPPs characterized by us were found to exhibit mostly saddle-type distortions.[13b]

A further indication for the ease in which conformationally similar porphyrins can form cocrystals was found with the regioisomeric mixture NiL[17]/NiL[18] that formed single crystals. The structure of the mixture (0.6:0.4 ratio, not shown) is slightly more non-planar than NiL[16] and exhibits conformational parameters quite similar to that of NiL[4] (Δ24 = 0.49 Å, δC_m = 0.14–0.23 Å, δC_b = 0.71–1.08 Å).[13b] These structures present the first examples of a 5,10,15,20-tetraarylporphyrin bearing five β-substituents.

Besides saddle distorted porphyrins like H_2L^6, tetraalkylporphyrins with bulky *meso*-substituents have been shown to be non-planar.[27–29] Notably, the tetra(*tert*-butyl)porphyrin H_2L^{24} exhibits a very ruffled conformation.[27,29] In order to obtain a monofunctionalized series of porphyrins potentially possessing various degrees of ruffling we attempted the formylation of the nickel(II) complexes of H_2L^{20}–H_2L^{23}.[28] While formylation is easily achieved, acceptable yields were obtained only for NiL[26] and NiL[28]. Formylation of *n*-butyl and isopropyl derivatives gave NiL[25] and NiL[27] in less than 20% yield. The remainder of the starting material was converted into a complex mixture of yet unidentified red-brown products. Spectroscopic analyses of the formylporphyrins showed a bathochromic shift of about 20 nm compared to the educts. The spectroscopic characteristics of the porphyrins NiL[25]–NiL[28] were quite similar to each other, indicating closely related conformations in solution. As of yet we have been unable to grow suitable crystals of any of these formylporphyrins and thus cannot provide conclusive data on their conformation.

We also attempted the perbromination of the *meso*-alkylporphyrins H_2L^{20}–H_2L^{24} in analogy to the reactions described above for the conversion of *meso*-tetraarylporphyrins into octabromotetraarylporphyrins. Exploratory experiments showed the reactions to be quite complex and satisfactory analytical data for a completely brominated product NiL[29] were obtained only from the bromination reaction of NiL[23]. Here, the main problem is the formation of mixtures of partially brominated products and reactions involving the alkyl substituents as has been noted by Wijesekera *et al.*[30] during their work on the bromination of *meso*-perfluoroalkyl porphyrins.

Currently we are utilizing the compounds described here for various coupling reactions and will report on these studies in due course.

Experimental

General experimental conditions and techniques were as described earlier.[12] The free base porphyrins were synthesized as described earlier by us (H_2L^1–H_2L^6,[13a] H_2L^{20}–H_2L^{24}[29]); H_2L^7 was synthesized according to the literature.[23]

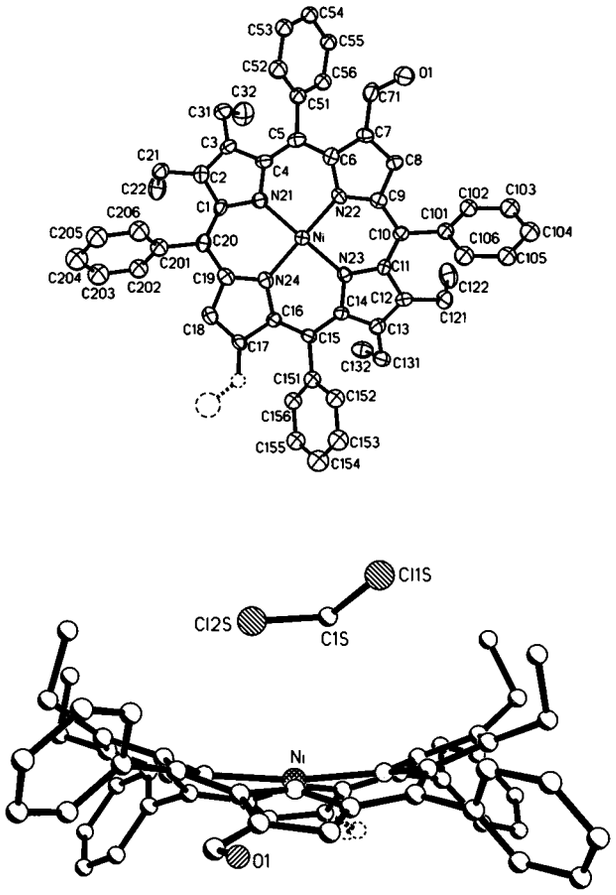

Fig. 8 Computer generated view (top) of the molecular structure of the monoclinic modification of NiL^{16} in the crystal. Hydrogen atoms have been omitted for clarity and thermal ellipsoids are drawn for 50% occupancy. Dashed lines indicate the minor formyl orientation. The side view (bottom) illustrates the incorporation of a methylene chloride of solvation in the binding pocket.

Syntheses

2,13-Dibromo-7,8-diethyl-5,10,15,20-tetraphenylporphyrin H_2L^9. Free base porphyrin H_2L^2 (300 mg, 0.45 mmol) and 80 mg (0.45 mmol, 1 equivalent) *N*-bromosuccinimide were dissolved in 100 ml dry chloroform and heated under reflux for 1 h. Another portion of 80 mg NBS was added and heating under reflux continued for 1 h. Monitoring by TLC showed the formation of several products. The reaction mixture was cooled to room temperature and the solvent removed with a rotary evaporator. The residue was taken up in a small amount of dichloromethane and filtered through neutral alumina (Brockmann grade III). Column chromatographic separation on alumina (grade III) with dichloromethane–*n*-hexane (1 : 1, v/v) yielded two main fractions each of which appeared to contain three different compounds (TLC). Despite repeated attempts, including the use of HPLC, only one pure compound could be isolated from the first column chromatographic fraction. Rechromatography of this fraction on silica gel eluting with dichloromethane–*n*-hexane (2 : 3, v/v), followed by recrystallization from dichloromethane–methanol, yielded purple crystals of H_2L^9. Yield 15 mg (20 μmol), 4%, mp > 300 °C (Found: C, 69.39; H, 4.79; N, 6.47. $C_{24}H_{18}BrN_2 \cdot H_2O$ requires C, 69.58; H, 4.38; N, 6.76%); δ_H (250 MHz, $CDCl_3$, TMS) −3.2 (s, 1H, NH), −2.3 (s, 1H, NH), 0.85 (t, 6H, CH_3), 2.8 (q, 4H, CH_2CH_3), 7.65–7.85 (m, 12H, aromatic $H_{m,p}$), 8.1–8.25 (m, 8H, aromatic H_o), 8.45 (s, 2H, β-H) and 8.7 (s, 2H, β-H); *m*/*z* (80 eV, 350 °C) 828 (M^+, 50), 750 ($M^+ - Br$, 31) and 670 ($M^+ - 2Br$, 100%); λ_{max}/nm (log ε/dm^3 mol^{-1} cm^{-1}) (CH_2Cl_2) 430 (5.54), 530 (4.17), 599 (3.48) and 657 (3.71).

2,12-Dibromo-7,8-diethyl-5,10,15,20-tetraphenylporphyrin H_2L^{10}. Free base porphyrin H_2L^2 (300 mg, 0.45 mmol) and 80 mg (0.45 mmol, 1 equivalent) NBS were dissolved in 100 ml dry chloroform and heated under reflux for 3 h. Again, TLC control showed the formation of several products of which only one compound could be obtained in pure form. After work-up and column chromatography on alumina as described for H_2L^9 the first fraction was rechromatographed on silica gel eluting with dichloromethane–*n*-hexane (1 : 1, v/v), followed by recrystallization from dichloromethane–methanol yielded purple crystals of H_2L^{10}. Yield 20 mg (30 μmol), 6%, mp > 300 °C (Found: C, 69.73; H, 4.47; N, 6.52. $C_{24}H_{18}BrN_2$ requires C, 69.58; H, 4.38; N, 6.76%); δ_H (250 MHz, $CDCl_3$, TMS) −3.0 (s, 1H, NH), −2.32 (s, 1H, NH), 0.66 (t, 3H, CH_3), 0.82 (t, 3H, CH_3), 2.56–2.8 (m, 4H, CH_2CH_3), 7.66–7.82 (m, 12H, aromatic $H_{m,p}$), 8.12–8.28 (m, 8H, aromatic H_o), 8.4 (s, 1H, β-H), 8.48 (s, 1H, β-H) and 8.74 (d, 2H, β-H); *m*/*z* (80 eV, 300 °C) 750 ($M^+ - Br$, 38), 670 ($M^+ - 2Br$, 93) and 414 (M^{2+}, 11%); λ_{max}/nm (log ε/dm^3 mol^{-1} cm^{-1}) (CH_2Cl_2) 434 (5.33), 533 (4.11), 601 (3.81) and 660 (3.89).

2,3,6,7,8,12,13-Hexabromo-17,18-diethyl-5,10,15,20-tetraphenylporphyrin H_2L^{12}. A three necked flask equipped with a condenser, dropping funnel and drying tube was charged with a solution of 40 mg (0.06 mmol) ZnL^2 in 10 ml chloroform–tetrachloromethane (1 : 1, v/v). Over the course of 30 min a solution of 0.1 ml Br_2 in 6 ml solvent mixture ($CHCl_3$–CCl_4, 1 : 1) was added dropwise under stirring. The reaction mixture was stirred for 4 h followed by dropwise addition of 0.3 ml pyridine in 10 ml of the chlorinated solvent mixture. Stirring was continued for 12 h followed by quenching of excess of bromine with a 20% aqueous solution of sodium disulfite. The phases were separated in a separatory funnel and the aqueous phase extracted with dichloromethane. The combined organic phases were concentrated on a rotary evaporator and filtered through neutral alumina (deactivated, grade III). Column chromatography on alumina grade III with dichloromethane–*n*-hexane (1 : 1, v/v), followed by recrystallization from dichloromethane–methanol, gave dark green crystals of H_2L^{12}. Yield 30 mg (30 μmol), 48%, mp > 300 °C (Found: C, 50.53; H, 2.75; N, 4.43. $C_{24}H_{16}Br_3N_2$ requires C, 50.39; H, 2.82; N 4.9%); δ_H (250 MHz, $CDCl_3$, TMS) −2.15 (s, 2H, NH), 0.55 (t, 6H, CH_3), 2.2–2.45 (m, 2H, CH_2CH_3), 2.6–2.8 (m, 2H, CH_2CH_3), 7.7–7.85 (m, 12H, aromatic $H_{m,p}$) and 8.15–8.35 (m, 8H, aromatic H_o); *m*/*z* (80 eV, 350 °C) 1146 ($M^+ + 2H$, 2), 1066 ($M^+ - Br$, 2), 988 ($M^+ - 2Br$, 2), 908 ($M^+ - 3Br$, 2) and 664 (100%); λ_{max}/nm (log ε/dm^3 mol^{-1} cm^{-1}) (CH_2Cl_2) 467 (5.21), 574 (3.57), 626 (3.52) and 732 (3.48).

2,3,12,13-Tetrabromo-7,8,17,18-tetraethyl-5,10,15,20-tetraphenylporphyrin H_2L^{13}. Following the procedure described for H_2L^{12}, 20 mg NiL^3 (0.03 mmol) in 16 ml solvent mixture were treated with 0.1 ml Br_2 in 10 ml solvent mixture and 0.3 ml pyridine in 10 ml solvent mixture. Yield 10 mg (10 μmol) green crystals, 38%, mp > 300 °C (Found: C, 59.80; H, 3.99; N, 5.46. $C_{26}H_{21}Br_2N_2$ requires C, 59.91; H, 4.06; N, 5.37%); δ_H (250 MHz, $CDCl_3$, TMS) −2.4 (s, 2H, NH), 0.6 (t, 12H, CH_3), 2.25–2.5 (m, 4H, CH_2CH_3), 2.6–2.8 (m, 4H, CH_2CH_3), 7.65–7.8 (m, 12H, aromatic $H_{m,p}$) and 8.15–8.25 (m, 8H, aromatic H_o); *m*/*z* (80 eV, 380 °C) 1044 ($M^+ + 2H$, 100), 968 ($M^+ - Br$, 78), 886 ($M^+ + 2H - 2Br$, 48), 806 ($M^+ - 3Br$, 24) and 726 ($M^+ - 4Br$, 22%); λ_{max}/nm (log ε/dm^3 mol^{-1} cm^{-1}) (CH_2Cl_2) 462 (5.52), 569 (4.10), 625 (3.69) and 722 (4.15).

2,3,7,8-Tetrabromo-12,13,17,18-tetraethyl-5,10,15,20-tetraphenylporphyrin H_2L^{14}. Following the procedure described for H_2L^{12}, 100 mg NiL^4 (0.13 mmol) in 16 ml solvent mixture were treated with 0.2 ml Br_2 in 14 ml solvent mixture and 0.6 ml pyridine in 14 ml solvent mixture. Yield 70 mg (70 μmol) green crystals, 53%, mp > 300 °C (Found: C, 59.75; H, 4.17; N, 5.12.

$C_{26}H_{21}Br_2N_2$ requires C, 59.91; H, 4.06; N, 5.37%); δ_H (250 MHz, $CDCl_3$, TMS) −1.52 (br s, 2H, NH), 0.36 (t, 6H, CH_3), 0.58 (t 6H, CH_3), 1.86–2.08 (m, 2H, CH_2CH_3), 2.12–2.32 (m, 2H, CH_2CH_3), 2.44–2.64 (m, 4H, CH_2CH_3), 7.68–7.88 (m, 12H, aromatic $H_{m,p}$) and 8.2–8.4 (m, 8H, aromatic H_o); *m*/*z* (80 eV, 300 °C) 1042 (M^+, 63), 964 ($M^+ - Br$, 100), 884 ($M^+ - 2Br$, 89), 804 ($M^+ - 3Br$, 34) and 725 ($M^+ - 4Br$, 15%); λ_{max}/nm (log ε/dm^3 mol^{-1} cm^{-1}) (CH_2Cl_2) 466 (5.23), 569 (3.98), 619 (4.07) and 726 (4.04).

2,3-Dibromo-7,8,12,13,17,18-hexaethyl-5,10,15,20-tetraphenylporphyrin H_2L[15]. Following the procedure described for H_2L[12], 50 mg NiL[5] (0.06 mmol) in 16 ml solvent mixture were treated with 0.1 ml Br_2 in 10 ml solvent mixture and 0.3 ml pyridine in 10 ml solvent mixture. Yield 30 mg (30 μmol) green crystals, 54%, mp 287 °C (Found: C, 71.53; H, 5.51; N, 5.87. $C_{28}H_{26}BrN_2$ requires C, 71.49; H, 5.57; N, 5.96%); δ_H (250 MHz, $CDCl_3$, TMS) −2.25 (br s, 2H, NH), 0.2–0.4 (m, 6H, CH_3), 0.45–0.75 (m, 12H, CH_3), 2.2–2.75 (m, 12H, CH_2CH_3), 7.6–7.8 (m, 12H, aromatic $H_{m,p}$) and 8.2–8.4 (m, 8H, aromatic H_o); *m*/*z* (80 eV, 350 °C) 942 ($M^+ + 2H$, 28), 862 ($M^+ - Br$, 100) and 784 ($M^+ - 2Br$, 51%); λ_{max}/nm (log ε/dm^3 mol^{-1} cm^{-1}) (CH_2Cl_2) 458 (5.40), 560 (4.21), 614 (4.06) and 711 (4.12).

Metallation

Zinc(II) insertion was performed in methylene chloride using the acetate method.[31] Metallation with nickel(II) acetate proceeded slowly and in low yields. Thus, nickel(II) acetylacetonate was used as metallation agent. The porphyrin free bases were dissolved in a small amount of toluene and treated with an excess of nickel(II) acetylacetonate. The mixture was heated to reflux until TLC control showed completion of the reaction. After removal of solvent *in vacuo* the residue was taken up in dichloromethane and filtered through neutral alumina (Brockmann grade III). The eluate was concentrated, layered with methanol and crystals could generally be obtained within a few days.

(2,3,7,8,12,13-Hexabromo-17,18-diethyl-5,10,15,20-tetraphenylporphyrinato)zinc(II) ZnL[12]. Yield 40 mg (30 μmol) blue-green crystals, 76%, mp > 300 °C (Found: C, 47.84; H, 2.42; N, 4.75. $C_{48}H_{30}Br_3N_2Zn$ requires C, 47.74; H, 2.5; N, 4.64%); δ_H (250 MHz, $CDCl_3$, TMS), 0.5 (t, 6H, CH_3), 2.35 (br s, 4H, CH_2CH_3), 7.65–7.8 (m, 12H, aromatic $H_{m,p}$) and 8.05–8.25 (m, 8H, aromatic H_o); *m*/*z* (80 eV, 380 °C) 1207 (M^+, 100) and 1127 ($M^+ - Br$, 90%); λ_{max}/nm (log ε/dm^3 mol^{-1} cm^{-1}) (CH_2Cl_2) 467 (5.22), 608 (3.96) and 659 (3.97).

(2,3,7,8,12,13-Hexabromo-17,18-diethyl-5,10,15,20-tetraphenylporphyrinato)nickel(II) NiL[12]. Yield 21 mg (20 μmol), 68%, mp > 300 °C (Found: C, 48.25; H, 2.27; N, 4.77. $C_{48}H_{30}Br_6N_4Ni$ requires C, 48.0; H, 2.52; N, 4.67%); δ_H (250 MHz, $CDCl_3$, TMS) 0.5 (t, 6H, CH_3), 2.25 (br s, 4H, CH_2CH_3), 7.6–7.75 (m, 12H, aromatic $H_{m,p}$) and 7.9–8.0 (m, 8H, aromatic H_o); *m*/*z* (80 eV, 350 °C) 1200 (M^+, 20), 1122 ($M^+ - Br$, 7), 1042 ($M^+ - 2Br$, 5), 962 ($M^+ - 3Br$, 4), 882 ($M^+ - 4Br$, 5), 798 ($M^+ - 5Br$, 6), 718 ($M^+ - 6Br$, 33) and 80 (Br, 100%); λ_{max}/nm (log ε/dm^3 mol^{-1} cm^{-1}) (CH_2Cl_2) 445 (5.40), 560 (4.27) and 601 (4.04).

(2,3,12,13-Tetrabromo-7,8,17,18-tetraethyl-5,10,15,20-tetraphenylporphyrinato)nickel(II) NiL[13]. Yield 7 mg (6 μmol), 67%, mp 296 °C (Found: C, 56.89; H, 3.57; N, 5.15. $C_{52}H_{40}Br_4N_4Ni$ requires C, 56.82; H, 3.67; N, 5.10%); δ_H (250 MHz, $CDCl_3$, TMS) 0.4–0.55 (s, 12H, CH_3), 2.25 (br s, 8H, CH_2CH_3), 7.6–7.75 (m, 12H, aromatic $H_{m,p}$), and 7.9–8.05 (m, 8H, aromatic H_o); *m*/*z* (80 eV, 380 °C) 1099 (M^+, 100), 1021 ($M^+ - Br$, 25), 943 ($M^+ - 2Br$, 19), 863 ($M^+ - 3Br$, 16) and 785 ($M^+ - 4Br$, 31%); λ_{max}/nm (log ε/dm^3 mol^{-1} cm^{-1}) (CH_2Cl_2) 443 (5.35), 559 (4.24) and 593 (3.94).

(2,3,7,8-Tetrabromo-12,13,17,18-diethyl-5,10,15,20-tetraphenylporphyrinato)nickel(II) NiL[14]. Yield 20 mg (20 μmol), 63%, mp > 297 °C (Found: C, 56.96; H, 3.55; N, 5.21. $C_{52}H_{40}Br_4N_4Ni$ requires C, 56.82; H, 3.67; N, 5.10%); δ_H (250 MHz, $CDCl_3$, TMS) 0.4–0.55 (m, 12H, CH_3), 2.25 (br s, 8H, CH_2CH_3), 7.55–7.75 (m, 12H, aromatic $H_{m,p}$) and 7.9–8.05 (m, 8H, aromatic H_o); *m*/*z* (80 eV, 380 °C) 1098 (M^+, 100), 1020 ($M^+ - Br$, 26), 940 ($M^+ - 2Br$, 25), 862 ($M^+ - 3Br$, 24), 784 ($M^+ - 4Br$, 96) and 549 (M^{2+}, 7%); λ_{max}/nm (log ε/dm^3 mol^{-1} cm^{-1}) (CH_2Cl_2) 442 (5.38), 557 (4.21) and 594 (3.94).

(2,3-Dibromo-7,8,12,13,17,18-hexaaethyl-5,10,15,20-tetraphenylporphyrinato)nickel(II) NiL[15]. Yield 20 mg (20 μmol), 95%, mp > 300 °C (Found: C, 67.03; H, 5.22; N, 5.39. $C_{56}H_{50}Br_2N_4Ni$ requires C, 67.43; H, 5.05; N, 5.62%), δ_H (250 MHz, $CDCl_3$, TMS) 0.4–0.6 (m, 18H, CH_3), 2.25 (br s, 12H, CH_2CH_3), 7.5–7.75 (m, 12H, aromatic $H_{m,p}$) and 7.95–8.1 (m, 8H, aromatic H_o); *m*/*z* (80 eV, 320 °C) 996 (M^+, 100), 918 ($M^+ - Br$, 13), 840 ($M^+ - 2Br$, 43), 812 ($M^+ - 2Br - C_2H_4$, 20) and 498 (M^{2+}, 7%); λ_{max}/nm (log ε/dm^3 mol^{-1} cm^{-1}) (CH_2Cl_2) 437 (5.42), 555 (4.21) and 599 (4.13).

Vilsmeier formylation

A 250 ml three necked round bottom flask, equipped with a condenser, thermometer, dropping funnel and drying tube, was charged at 0 °C with an appropriate amount of DMF and $POCl_3$ and the mixture stirred for 30 min at room temperature. After formation of the Vilsmeier complex the mixture was diluted with a few ml of 1,2-dichloroethane and a solution of the porphyrin in 1,2-dichloroethane added dropwise. After complete addition of the porphyrin the solution was heated for 1 h at 55–60 °C (for nickel complexes of the β-ethyl-TPPs), 4 h for the nickel complexes of the tetraalkylporphyrins. Subsequently, the mixture was cooled with an ice–water bath and a saturated solution of sodium acetate in water added. The mixture was heated to reflux for 3 h, the phases separated and the aqueous phase extracted with dichloromethane. The organic phase was washed several times with water, concentrated with a rotary evaporator and filtered through neutral alumina (grade III). The crude product mixture was purified by column chromatography on neutral alumina (grade III) with dichloromethane–*n*-hexane (1 : 1, v/v). The product fraction was recrystallized from dichloromethane–methanol.

(2,3,12,13-Tetraethyl-7-formyl-5,10,15,20-tetraphenylporphyrinato)nickel(II) NiL[16]. The complex NiL[3] (15 mg, 0.02 mmol) was dissolved in 10 ml dichloroethane and added to the Vilsmeier complex formed from 1 ml $POCl_3$ and 1 ml DMF in 4 ml dichloroethane as described above. Yield 10 mg (10 μmol), 66%, mp > 300 °C (Found: C, 78.33; H, 5.32; N, 6.97. $C_{53}H_{44}N_4NiO$ requires C, 78.43; H, 5.46; N, 6.90%) δ_H (250 MHz, $CDCl_3$, TMS) 0.72–0.84 (m, 12H, CH_3), 2.42–2.62 (m, 8H, CH_2CH_3), 7.58–7.78 (m, 12H, aromatic $H_{m,p}$), 7.92–8.12 (m, 8H, aromatic H_o), 8.2–8.24 (d, 1H, β-H), 8.28–8.32 (d, 1H, β-H), 8.58 (s, 1H, β-H) and 8.78 (s, 1H, CHO); *m*/*z* (80 eV, 300 °C) 812 (M^+, 100), 783 ($M^+ - CHO$, 19) and 406 (M^{2+}, 8%); λ_{max}/nm (log ε/dm^3 mol^{-1} cm^{-1}) (CH_2Cl_2) 438 (5.19), 554 (4.12) and 608 (4.21).

(2,3,7,8,12,13-Hexaethyl-17-formyl-5,10,15,20-tetraphenylporphyrinato)nickel(II) NiL[19]. The complex NiL[5] (100 mg, 0.12 mmol) was dissolved in 20 ml dichloroethane and added to the Vilsmeier complex formed from 2 ml $POCl_3$ and 2 ml DMF in 5 ml dichloroethane as described above. Yield 80 mg (90 μmol), 78%, mp > 300 °C (Found: C, 78.69; H, 5.99; N, 6.33. $C_{57}H_{52}N_4NiO$ requires C, 78.89; H, 6.04; N, 6.64%); δ_H (250 MHz, $CDCl_3$, TMS) 0.4–0.56 (m, 12H, CH_3), 0.6–0.72 (m, 6H, CH_3), 2.12–2.32 (m, 8H, CH_2CH_3), 2.4–2.52 (m, 4H, CH_2CH_3), 7.56–7.76 (m, 12H, aromatic $H_{m,p}$), 8.0–8.16 (m, 8H, aromatic H_o),

8.6 (s, 1H, β-H) and 8.64 (s, 1H, CHO); *m/z* (80 eV, 300 °C) 866 (M^+, 100), 838 ($M^+ - CHO$, 6) and 433 (M^{2+}, 9%); λ_{max}/nm (log ε/dm^3 mol^{-1} cm^{-1}) (CH_2Cl_2) 444 (5.25), 561 (4.12) and 613 (4.21).

(5,10,15,20-Tetrabutyl-2-formylporphyrinato)nickel(II) NiL[25]. The complex NiL[20] (250 mg, 0.42 mmol) was dissolved in 25 ml dichloroethane and added to the Vilsmeier complex formed from 7 ml $POCl_3$ and 7 ml DMF in 15 ml dichloroethane as described above. Yield 40 mg (70 μmol), 15%, mp 105 °C (Found: C, 71.36; H, 7.02; N, 8.87. $C_{37}H_{44}N_4NiO$ requires C, 71.74; H, 7.16; N, 9.04%); δ_H (250 MHz, $CDCl_3$, TMS) 0.86–1.0 (m, 12H, CH_3), 1.36–1.58 (m, 8H, CH_2CH_2-CH_3), 1.9–2.2 (m, 8H, $CH_2CH_2CH_3$), 9.0–9.16 (m, 6H, β-H), 9.7 (s, 1H, β-H) and 11.12 (s, 1H, CHO); *m/z* (80 eV, 100 °C) 618 (M^+, 100), 575 ($M^+ - C_3H_7$, 38), 547 ($M^+ - C_5H_{11}$, 10) and 309 (M^{2+}, 5%); λ_{max}/nm (log ε/dm^3 mol^{-1} cm^{-1}) (CH_2Cl_2) 437 (5.09), 556 (3.80) and 600 (3.76).

[2-Formyl-5,10,15,20-tetrakis(2-methylpropyl)porphyrinato]nickel(II) NiL[26]. The complex NiL[21] (100 mg, 0.17 mmol) was dissolved in 25 ml dichloroethane and added to the Vilsmeier complex formed from 2 ml $POCl_3$ and 2 ml DMF in 5 ml dichloroethane as described above. Yield 70 mg (0.17 mmol), 67%, mp 153 °C (Found: C, 71.62; H, 7.35; N, 9.39. $C_{37}H_{44}N_4$-NiO requires C, 71.74; H, 7.16; N, 9.04%); δ_H (250 MHz, $CDCl_3$, TMS) 0.55 [d, 6H, $CH_2CH(CH_3)_2$], 0.65–0.9 [m, 18H, $CH_2CH(CH_3)_2$], 1.8–1.95 [m, 1H, $CH_2CH(CH_3)_2$], 2.0–2.2 [m, 3H, $CH_2CH(CH_3)_2$], 4.3–4.55 [m, 8H, $CH_2CH(CH_3)_2$], 9.05–9.2 (m, 4H, β-H), 9.25 (d, 2H, β-H), 9.8 (s, 1H, β-H) and 11.25 (s, 1H, CHO); *m/z* (80 eV, 250 °C) 618 (M^+, 100), 590 ($M^+ - CO$, 13), 575 ($M^+ - C_3H_7$, 65) and 309 (M^{2+}, 12%); λ_{max}/nm (log ε/dm^3 mol^{-1} cm^{-1}) (CH_2Cl_2) 437 (5.27), 557 (3.92) and 601 (3.90).

(2-Formyl-5,10,15,20-tetraisopropylporphyrinato)nickel(II) NiL[27]. The complex NiL[22] (250 mg, 0.47 mmol) was dissolved in 25 ml dichloroethane and added to the Vilsmeier complex formed from 7 ml $POCl_3$ and 7 ml DMF in 15 ml dichloroethane as described above. Yield 50 mg (90 μmol), 19%, mp 288 °C (Found: C, 70.57; H, 6.12; N, 10.28. $C_{33}H_{36}N_4NiO$ requires C, 70.36; H, 6.44; N, 9.95%); δ_H (250 MHz, $CDCl_3$, TMS) 2.0 [d, 6H, $CH(CH_3)_2$], 2.1 [t, 18H, $CH(CH_3)_2$], 4.5–4.78 [m, 4H, $CH(CH_3)_2$], 9.08–9.16 (m, 5H, β-H), 9.28 (d, 1H, β-H), 9.82 (s, 1H, β-H) and 11.24 (s, 1H, CHO); *m/z* (80 eV, 300 °C) 562 (M^+, 100), 547 ($M^+ - CH_3$, 28), 519 ($M^+ - C_3H_7$, 11) and 281 (M^{2+}, 11%); λ_{max}/nm (log ε/dm^3 mol^{-1} cm^{-1}) (CH_2Cl_2) 441 (4.98), 565 (3.79) and 609 (3.75).

[5,10,15,20-Tetrakis(1-ethylpropyl)-2-formylporphyrinato]nickel(II) NiL[28]. The complex NiL[23] (200 mg, 0.31 mmol) was dissolved in 20 ml dichloroethane and added to the Vilsmeier complex formed from 4 ml $POCl_3$ and 4 ml DMF in 8 ml dichloroethane as described above. Yield 180 mg (27 mmol), 87%, mp > 300 °C (Found: C, 72.71; H, 7.48; N, 8.54. $C_{41}H_{52}N_4NiO$ requires C, 72.89; H, 7.76; N, 8.29%); δ_H (250 MHz, $CDCl_3$, TMS) 0.78 [t, 6H, $CH(CH_2CH_3)_2$], 0.9–1.0 [m, 18H, $CH(CH_2CH_3)_2$], 2.45–2.78 [m, 16H, $CH(CH_2CH_3)_2$], 4.05–4.3 [m, 4H, $CH(CH_2CH_3)_2$], 9.13–9.3 (m, 7H, β-H), 9.9 (s, 1H, β-H) and 11.33 (s, 1H, CHO); *m/z* (80 eV, 300 °C) 674 (M^+, 100), 645 ($M^+ - C_2H_5$, 41) and 337 (M^{2+}, 5%); λ_{max}/nm (log ε/dm^3 mol^{-1} cm^{-1}) (CH_2Cl_2) 440 (4.92), 562 (4.04) and 608 (3.99).

[2,3,7,8,12,13,17,18-Octabromo-5,10,15,20-tetrakis(1-ethylpropyl)porphyrinato]nickel(II) NiL[29]. The nickel(II) porphyrin NiL[23] (250 mg, 0.4 mmol) was dissolved in 100 ml dry chloroform and treated dropwise with a solution of 1g bromine (12.5 mmol) in 40 ml chloroform. The solution was stirred for 4 h and then diluted dropwise with 1.5 ml pyridine in 40 ml chloroform. Stirring was continued for 12 h, followed by addition of 100 ml sodium disulfite solution. The organic phase was separated, dried with sodium sulfate, concentrated and chromatographed on silica gel eluting with *n*-hexane. The first, dark brown to black fraction was collected and recrystallized. Yield 0.14 g (0.11 mmol), 28% green-blue crystals from CH_2Cl_2–*n*-hexane; mp > 300 °C (Found: C, 37.22; H, 3.23; N, 4.01. $C_{40}H_{44}Br_8N_4Ni$ requires C, 37.57; H, 3.46; N, 4.38%); δ_H (250 MHz, $CDCl_3$, TMS) 0.98–1.07 [3 × t, J = 7.4 Hz, 18H, $CH(CH_2CH_3)_2$], 1.19–1.25 [t, J = 7.0, 6H, $CH(CH_2CH_3)_2$], 1.80–2.53 [m, 16H, $CH(CH_2$-$CH_3)_2$] and 3.72–3.85 [qnt, J = 7.4 Hz, 4H, $CH(CH_2CH_3)_2$]; *m/z* (70 eV) 1277 (M^+, 16), 1206 [$M^+ - CH(CH_2CH_3)_2$, 100], 1127 ($M^+ - Br$, 37), 1047 ($M^+ - Br_2$, 28), 969 ($M^+ - Br_3$, 16) and 889 ($M^+ - Br_4$, 10%); λ_{max}/nm (log ε/dm^3 mol^{-1} cm^{-1}) (CH_2Cl_2) 231 (4.51), 360 (4.10), 477 (4.71) and 582 (4.43) [Found (HRMS): *m/z* 1277.6304. $C_{40}H_{44}Br_8N_4Ni$ requires 127.6341].

Crystallography

General. The crystals were immersed in hydrocarbon oil (Paraton N®), suitable single crystals selected under the microscope, mounted on a glass fiber and placed in the low-temperature N_2 stream on the diffractometer.[32] Intensity data for H_2L^7 were collected with a Syntex $P2_1$ instrument using graphite filtered Cu-Kα radiation (λ = 1.54178 Å) at 129 K with 2θ–θ scans while data for $[H_4L^{14}][CF_3CO_2]_2$, the two triclinic solvates of H_2L^{12}, $[H_4L^{12}][CF_3CO_2]_2$, and the triclinic and monoclinic modification of NiL[16] were collected at 130 K using a Siemens P4 diffractometer equipped with a rotating anode (2θ–θ scans, Ni-filtered Cu-Kα radiation, λ = 1.54178 Å). The intensities were corrected for Lorentz-polarization effects. Absorption corrections were applied using the program XABS 2;[33] extinction effects were disregarded. The data sets for the two modifications of H_2L^9 and H_2L^{10} were collected at 150 K using a Siemens SMART system complete with 3-circle goniometer and CCD detector utilizing Mo-Kα radiation (λ = 0.71073 Å). The data collection nominally covered a hemisphere of reciprocal space, by a combination of three sets of exposures: each set had a different φ angle, and each exposure covered 0.3° in ω. Repeating the initial frames at the end of the data collection and analysing the duplicate reflections monitored crystal decay. No decay was observed during all three data collections. The intensities were corrected for Lorentz-polarization effects. An absorption correction for the CCD data sets was applied using the program SADABS.[34] The structures of the free base porphyrins were solved with direct methods using the SHELXS 97 program[35] while the structures of the metalloporphyrins were solved *via* Patterson syntheses followed by structure expansion. Refinements were carried out by full-matrix least squares on $|F^2|$ with the program SHELXL 97 using all data.[36] Unless otherwise stated, non-hydrogen atoms were refined with anisotropic thermal parameters. Except for disordered groups, hydrogen atoms were generally placed into geometrically calculated positions and refined using a riding model. Some details of the crystal data and refinements are listed in Table 3.

Refinements. For the structures H_2L^7, H_2L^{12} (triclinic A), $[H_4L^{12}][CF_3CO_2]_2$ and NiL[16] (monoclinic modification) the phenyl rings were refined as rigid hexagons with isotropic thermal parameters. In most cases no hydrogen atoms were included for disordered positions. For H_2L^7 the bromine substituents were disordered over three sets of positions and refined with the following occupancies: Br1 0.36, Br2 0.56, Br3 0.08. Hydrogen atoms were added to all four pyrrole nitrogen atoms and refined with occupancies of 0.5, each. For H_2L^9 (monoclinic modification) the residual electron density is located close to Br1 (0.97 Å). For H_2L^{12} (triclinic A) hydrogen atoms were added to all four pyrrole nitrogen atoms and refined with 50% occupancy, each. Considerable disorder was found for

Table 3 Crystal and refinement data for the crystal structure determinations

		H_2L^9			H_2L^{12}				NiL[16]	
	H_2L^7	Orthorhombic	Monoclinic	H_2L^{10}	Triclinic A	Triclinic B	$[H_4L^{12}][CF_3CO_2]_2$	$[H_4L^{14}][CF_3CO_2]_2$	Triclinic	Monoclinic
Formula	$C_{44}H_{28}Br_2N_4$	$C_{48}H_{36}Br_2N_4$	$C_{48}H_{36}Br_2N_4$	$C_{48}H_{36}Br_2N_4$	$C_{48}H_{36}Br_6N_4 \cdot C_6H_{12}$	$C_{48}H_{36}Br_6N_4 \cdot 2CH_2Cl_2$	$[C_{48}H_{34}Br_6N_4]$-$[C_2F_3O_2]_2 \cdot 2CHCl_3$	$[C_{52}H_{44}Br_4N_4]$-$[C_2F_3O_2]_2 \cdot 2CHCl_3 \cdot 2CH_3OH$	$C_{53}H_{44}N_4NiO \cdot 0.75CHCl_3 \cdot 0.25H_2O$	$C_{53}H_{44}N_4NiO \cdot CH_2Cl_2$
Crystallization	$CHCl_3$–*n*-hexane	CH_2Cl_2–*n*-hexane	CH_2Cl_2–CH_3OH	CH_2Cl_2–*n*-hexane	$CHCl_3$–cyclohexane	CH_2Cl_2–CH_3OH	$CHCl_3$–CH_3OH + 1% TFA	$CHCl_3$–CH_3OH + 1% TFA	$CHCl_3$–CH_3OH	CH_2Cl_2–CH_3OH
M	772.52	828.63	828.63	828.63	1228.39	1314.09	1611.03	1573.41	905.66	896.56
Lattice type	Monoclinic	Orthorhombic	Monoclinic	Triclinic	Triclinic	Triclinic	Orthorhombic	Monoclinic	Triclinic	Monoclinic
Space group	$P2_1/n$	$P2_12_12_1$	$P2_1/n$	$P\bar{1}$	$P\bar{1}$	$P\bar{1}$	*Pnma*	*C*2/*c*	$P\bar{1}$	$P2_1/c$
a/Å	13.993(15)	7.1959(1)	11.8426(2)	9.9077(1)	13.309(10)	13.299(3)	15.803(9)	16.859(6)	12.579(3)	14.346(5)
b/Å	6.699(5)	20.2757(3)	14.1555(3)	14.0933	14.037(12)	17.047(4)	19.024(5)	19.710(11)	13.882(3)	13.803(5)
c/Å	18.832(17)	26.4499(1)	22.6044(2)	15.2952(2)	14.053(11)	22.967(5)	19.652(9)	20.042(7)	14.383(3)	22.890(10)
α/°				102.451(1)	105.43(6)	100.05(2)			86.40(2)	
β/°	100.41(8)		101.19	99.870(1)	93.42(6)	90.48(2)		103.27(3)	73.10(2)	104.43(3)
γ/°				107.814(1)	108.46(6)	106.56(2)			69.05(2)	
U/Å^3	1736(3)	3859.1(1)	3717.3(1)	1919.67(3)	2370(3)	4905(2)	5908(5)	6482(5)	2241.9(8)	4390(3)
Z	2	4	4	2	2	4	4	4	2	4
Reflections measured	2691	24458	22596	13309	6247	13486	4370	4003	6107	6375
Reflections unique	2321	9107	8740	8520	5935	12817	4046	3754	5935	5792
Reflections with $I > 2\sigma(I)$	1875	8435	6693	7256	4530	9332	2294	2619	3725	3375
R_{int}	0.1280	0.0281	0.0376	0.0204	0.0674	0.0471	0.0784	0.1180	0.0599	0.0843
μ/mm^{-1}	3.256	2.141	2.222	2.152	6.444	8.235	1.811	5.898	2.207	2.107
$R1$ (all data)	0.1306	0.0316	0.0681	0.050	0.1182	0.0913	0.1020	0.1394	0.1640	0.1578
$wR2$ (all data)	0.2771	0.0646	0.1242	0.1116	0.2487	0.1557	0.2106	0.2720	0.3280	0.2399
$R1$ [$I > 2\sigma(I)$]	0.1102	0.0275	0.0479	0.0406	0.0932	0.0602	0.0764	0.1008	0.1105	0.0876
$wR2$ [$I > 2\sigma(I)$]	0.2638	0.0628	0.1148	0.1063	0.2308	0.1386	0.1953	0.2428	0.2812	0.1965

the side chain bromine atoms and ethyl groups. This disorder could only be modeled by imposing rigid constraints. Three different sets of side chain placements were refined with the following occupancies: C21, C22, C31, C32 each 40% and Br2, Br3 each 60% at C2 and C3; C71, C72, C81, C82 each 30% and Br7, Br8 each 70% at C7 and C8; C171, C172, C181, C182 each 40% and Br17, Br18 each 60% at C17 and C18. In order to get a reasonably stable refinement all C–C units involving disordered groups were refined as rigid groups with fixed isotropic thermal parameters (0.03 for methylene groups, 0.04 for methyl groups). Nevertheless, despite all attempts significant shifts were always observed for the disordered carbon atoms. At best, the present structure can serve to illustrate the overall conformation of the macrocycle. No significance should be attributed to any individual geometrical parameters. For H_2L^{12} (triclinic B) Cl6S was refined as disordered over two split positions with occupancies of 0.75 (Cl6S) and 0.25 (Cl6′), respectively. Similarly, Cl8S was refined as disordered over two positions with occupancies of 0.8 (Cl8S) and 0.2 (Cl8′), respectively. One of the two porphyrin macrocycles in the asymmetric unit showed disorder of β-bromo and β-ethyl substituents. This disorder was modeled by employing two different sets of substituents: Br37, Br38, C271, C272, C281, and C282 were refined with occupancies of 0.2, each, while Br27, Br28, C371, C372, C381, and C382 were refined with occupancies of 0.8 each. This model employed severe constraints for the disordered ethyl groups; these were refined with isotropic thermal parameters of 0.03 for the methylene groups and 0.04 for the methyl groups. The residual electron density was located in the disordered substituent region. Owing to this disorder and the constraints imposed on molecule 2 only molecule 1 (containing N21) should be used for geometrical analyses. For $[H_4L^{12}][CF_3CO_2]_2$, with the exception of C31, C32, Cl1S, Cl1′, C2A, F2A and F1A, all other non-hydrogen atoms were refined with anisotropic thermal parameters. For the chloroform molecule containing C1S one chlorine atom was refined as disordered over two split positions (Cl1S and Cl1′) with equal occupancies. In addition, there was crystallographically required disorder in all counter anions and solvate molecules. A further problem was encountered with the two ethyl groups. Potentially a small amount of bromine ethyl disorder is encountered here since the large residual electron density is located about 1.8 Å apart from C2. In addition, all attempts failed to refine the ethyl carbon atoms by conventional means. In the end the only practical course was ignoring the residual electron density and refining the ethyl carbon atoms with a common isotropic thermal parameter. All other attempts failed to model this situation. For $[H_4L^{14}][C_2F_3O_2]_2$ the structure contained severely disordered trifluoroacetate anions, for which the fluorine atoms were refined with three split positions of equal occupancy. Owing to the limited number of reflections, phenyl C5 was refined as a rigid hexagon and only some side chain atoms were refined with anisotropic thermal parameters. The residual electron density is located near the bromine atoms. For NiL^{16} (monoclinic modification) the formyl group was found to be disordered over two positions (at C7 and C17) and was refined as disordered over two positions with occupancies of 0.8 and 0.2, respectively. The atom C1S in the solvate molecule showed relatively high thermal parameters.

CCDC reference number 186/1219.

See http://www.rsc.org/suppdata/dt/1998/4187/ for crystallographic files in .cif format.

Acknowledgements

This work was supported by grants from the Deutsche Forschungsgemeinschaft (Se543/2–4 and Heisenberg scholarship/3-1, M. O. S.), the Fonds der Chemischen Industrie (M. O. S.), Syracuse University (K. R.-S.), the Petroleum Research Fund, administered by the American Chemical Society (Grant ACS-PRF 28361-G3, K. R.-S.), and the National Science Foundation (CHE-97-02246, K. R.-S.). We gratefully acknowledge funds from the NSF (CHE-95-27898), the W. M. Keck Foundation, and Syracuse University which made possible purchase of the X-ray diffractometer at Syracuse University. We also acknowledge the co-operation of the UC Davis crystallographic facility (M. M. Olmstead, director) where we performed some of the data collections.

References

1 (*a*) K. M. Barkigia, L. Chantranupong, K. M. Smith and J. Fajer, *J. Am. Chem. Soc.*, 1988, **110**, 7566; (*b*) A. Forman, M. W. Renner, E. Fujita, K. M. Barkigia, M. C. W. Evans, K. M. Smith and J. Fajer, *Isr. J. Chem.*, 1989, **29**, 57; R. Huber, *Eur. J. Biochem.*, 1990, **187**, 283; J. Fajer, *Chem. Ind. (London)*, 1991, 869; M. O. Senge, *J. Photochem. Photobiol. B:Biol.*, 1992, **16**, 3; M. Ravikanth and T. K. Chandrashekar, *Struct. Bonding (Berlin)*, 1995, **82**, 105.

2 M. B. Hursthouse and S. Neidle, *J. Chem. Soc., Chem. Commun.*, 1972, 449; J.-H. Fuhrhop, L. Witte and W. S. Sheldrick, *Liebigs Ann. Chem.*, 1976, 1537.

3 (*a*) K. M. Barkigia, M. D. Berber, J. Fajer, C. J. Medforth, M. W. Renner and K. M. Smith, *J. Am. Chem. Soc.*, 1990, **112**, 8851; L. D. Sparks, C. J. Medforth, M.-S. Park, J. R. Chamberlain, M. R. Ondrias, M. O. Senge, K. M. Smith and J. A. Shelnutt, *J. Am. Chem. Soc.*, 1993, **115**, 581; J. A. Shelnutt, C. J. Medforth, M. D. Berber, K. M. Barkigia and K. M. Smith, *J. Am. Chem. Soc.*, 1991, **113**, 4077; M. O. Senge, C. J. Medforth, L. D. Sparks, J. A. Shelnutt and K. M. Smith, *Inorg. Chem.*, 1993, **32**, 1716; K. M. Barkigia, M. W. Renner, L. R. Furenlid, C. J. Medforth, K. M. Smith and J. Fajer, *J. Am. Chem. Soc.*, 1993, **115**, 3627; M. W. Renner, K. M. Barkigia, Y. Zhang, C. J. Medforth, K. M. Smith and J. Fajer, *J. Am. Chem. Soc.*, 1994, **116**, 8582; S. Gentemann, C. J. Medforth, T. P. Forsyth, D. J. Nurco, K. M. Smith, J. Fajer and D. Holten, *J. Am. Chem. Soc.*, 1994, **116**, 7363; M. W. Renner, K. M. Barkigia, D. Melamed, K. M. Smith and J. Fajer, *Inorg. Chem.*, 1996, **35**, 5120; L. D. Sparks, K. K. Anderson, C. J. Medforth, K. M. Smith and J. A. Shelnutt, *Inorg. Chem.*, 1994, **32**, 2297; K. M. Kadish, E. Van Caemelbecke, F. D'Souza, C. J. Medforth, K. M. Smith, A. Tabard and R. Guilard, *Inorg. Chem.*, 1995, **34**, 2984; M. O. Senge, W. W. Kalisch and S. Runge, *Liebigs Ann. Chem.*, 1997, 1345; (*b*) S. Gentemann, N. Y. Nelson, L. Jaquinod, D. J. Nurco, S. H. Leung, C. J. Medforth, K. M. Smith, J. Fajer and D. Holten, *J. Phys. Chem. B*, 1997, **101**, 1247; R.-J. Cheng, P.-Y. Chen, P.-R. Gau and S.-M. Peng, *J. Am. Chem. Soc.*, 1997, **119**, 2563; A. Regev, T. Galili, C. J. Medforth, K. M. Smith, K. M. Barkigia, J. Fajer and H. Levanon, *J. Phys. Chem.*, 1994, **99**, 2520

4 D. Mandon, P. Ochsenbein, J. Fischer, R. Weiss, K. Jayaraj, R. N. Austin, A. Gold, P. S. White, O. Brigaud, P. Battioni and D. Mansuy, *Inorg. Chem.*, 1992, **31**, 2044; P. Bhyrappa, V. Krishnan and M. Nethaji, *J. Chem. Soc., Dalton Trans.*, 1993, 1901; P. Ochsenbein, D. Mandon, J. Fischer, R. Weiss, R. Austin, K. Jayaraj, A. Gold, J. Terner, E. Bill, M. Müther and A. X. Trautwein, *Angew. Chem., Int. Ed. Engl.*, 1993, **32**, 1437; L. M. Henling, W. P. Schaefer, J. A. Hodge, M. E. Hughes and H. B. Gray, *Acta Crystallogr., Sect. C*, 1993, **49**, 1743; W. P. Schaefer, J. A. Hodge, M. E. Hughes, H. B. Gray, J. E. Lyons, P. E. Ellis, Jr. and R. W. Wagner, *Acta Crystallogr., Sect. C*, 1993, **49**, 1342; R. E. Marsh, W. P. Schaefer, J. A. Hodge, M. E. Hughes and H. B. Gray, *Acta Crystallogr., Sect. C*, 1993, **49**, 1339; E. R. Birnbaum, J. A. Hodge, M. W. Grinstaff, W. P. Schaefer, L. Henling, J. A. Labinger, J. E. Bercaw and H. B. Gray, *Inorg. Chem.*, 1995, **34**, 3625; M. W. Grinstaff, M. G. Hill, E. R. Birnbaum, W. P. Schaefer, J. A. Labinger and H. B. Gray, *Inorg. Chem.*, 1995, **34**, 4896; K. M. Kadish, J. Li, E. Van Caemelbecke, Z. Ou, N. Guo, M. Autret, F. D'Souza and P. Tagliatesta, *Inorg. Chem.*, 1997, **36**, 6292.

5 G. A. Spyroulias, A. Despotopoulos, C. P. Raptopoulou, A. Terzis and A. G. Coutsolelos, *Chem. Commun.*, 1997, 783.

6 P. Bhyrappa, M. Nethaji and V. Krishnan, *Chem. Lett.*, 1993, 869.

7 M. O. Senge, T. P. Forsyth, L. T. Nguyen and K. M. Smith, *Angew. Chem., Int. Ed. Engl.*, 1994, **33**, 2485.

8 P. E. Ellis Jr. and J. E. Lyons, *Coord. Chem. Rev.*, 1990, **105**, 181; B. Meunier, *Chem. Rev.*, 1992, **92**, 1411; J. E. Lyons and P. E. Ellis Jr., in *Metalloporphyrins in Catalytic Oxidations*, ed. R. A. Sheldon, Marcel Dekker, New York, 1994, p. 297; D. Dolphin, T. D. Traylor and L. Y. Xie, *Acc. Chem. Res.*, 1997, **30**, 251; M. W. Grinstaff, M. G. Hill, J. A. Labinger and H. B. Gray, *Science*, 1994, **264**, 1311; E. Baciocchi, T. Boschi, L. Cassioli, C. Galli, A. Lapi and P. Tagliatesta, *Tetrahedron Lett.*, 1997, **38**, 7283; F. D'Souza, Y.-Y. Hsieh and G. R. Deviprasad, *J. Electroanal. Chem., Interfacial Electrochem.*, 1997, **426**, 17.

9 D. Dolphin, *J. Heterocycl. Chem.*, 1970, **7**, 275; B. Evans, K. M. Smith and J.-H. Fuhrhop, *Tetrahedron Lett.*, 1977, **5**, 443; S. Tsuchiya, *Chem. Phys. Lett.*, 1990, **169**, 608; C. J. Medforth, M. D. Berber, K. M. Smith and J. A. Shelnutt, *Tetrahedron Lett.*, 1990, **31**, 3719.
10 (*a*) P. Bhyrappa and V. Krishnan, *Inorg. Chem.*, 1991, **30**, 239; (*b*) T. P. Wijesekera, A. Matsumoto, D. Dolphin and D. Lexa, *Angew. Chem., Int. Ed. Engl.*, 1990, **29**, 1028; T. P. Wijesekera, D. Dupré, M. S. R. Cader and D. Dolphin, *Bull. Soc. Chim. Fr.*, 1996, **133**, 765; M. S. Chorghade, D. Dolphin, D. Dupré, D. R. Hill, E. C. Lee and T. P. Wijesekera, *Synthesis*, 1996, 1320.
11 (*a*) K. S. Chan, X. Zhou, B.-S. Lou and T. C. W. Mak, *J. Chem. Soc., Chem. Commun.*, 1994, 271; (*b*) K. S. Chan, X. Zhou, M. T. Au and C. Y. Tam, *Tetrahedron*, 1995, **51**, 3129.
12 S. Runge and M. O. Senge, *Z. Naturforsch., Teil B*, 1998, **53b**, 1021.
13 (*a*) W. W. Kalisch and M. O. Senge, *Tetrahedron Lett.*, 1996, **37**, 1183; (*b*) M. O. Senge and W. W. Kalisch, *Inorg. Chem.*, 1997, **36**, 6103; (*c*) M. O. Senge, W. W. Kalisch and S. Runge, *Tetrahedron*, 1998, **54**, 3781.
14 H. Fischer and F. Lindner, *Hoppe-Seyler's Z. Physiol. Chem.*, 1926, **161**, 20; E. Samuels, R. Shuttleworth and T. S. Stevens, *J. Chem. Soc. C*, 1968, 145; T. Traylor and S. Tsuchiya, *Inorg. Chem.*, 1987, **26**, 1338.
15 H. C. Callot, *Tetrahedron Lett.*, 1973, 4987; *Bull. Soc. Chim. Fr.*, 1974, **8**, 1492.
16 P. Ochsenbein, K. Ayougou, D. Mandon, J. Fischer, R. Weiss, R. N. Austin, K. Jayaraj, A. Gold, J. Terner and J. Fajer, *Angew. Chem., Int. Ed. Engl.*, 1994, **33**, 348; J.-Z. Zou, M. Li, Z. Xu, X.-Z. You and H. Wang, *Huaxue Xuebao*, 1994, **52**, 683 (*Chem. Abstr.*, 1995, **122**, 22438p); J.-Z. Zou, Z. Xu, M. Li and X.-Z. You, *Acta Crystallogr., Sect. C*, 1995, **51**, 760; K. M. Kadish, M. Autret, Z. Ou, P. Tagliatesta, T. Boschi and V. Fares, *Inorg. Chem.*, 1997, **36**, 204.
17 W. R. Scheidt and Y. J. Lee, *Struct. Bonding (Berlin)*, 1987, **64**, 1.
18 W. Jentzen, X.-Z. Song and J. A. Shelnutt, *J. Phys. Chem. B*, 1997, **101**, 1684.
19 X.-Z. Song, W. Jentzen, S.-L. Jia, L. Jaquinod, D. J. Nurco, C. J. Medforth, K. M. Smith and J. A. Shelnutt, *J. Am. Chem. Soc.*, 1996, **118**, 12975.
20 M. O. Senge, C. J. Medforth, T. P. Forsyth, D. A. Lee, M. M. Olmstead, W. Jentzen, R. K. Pandey, J. A. Shelnutt and K. M. Smith, *Inorg. Chem.*, 1997, **36**, 1149.
21 D. J. Nurco, C. J. Medforth, T. P. Forsyth, M. M. Olmstead and K. M. Smith, *J. Am. Chem. Soc.*, 1996, **118**, 10918; K. M. Barkigia, D. J. Nurco, M. W. Renner, D. Melamed, K. M. Smith and J. Fajer, *J. Phys. Chem. B*, 1998, **102**, 322.
22 H. Duval, V. Bulach, J. Fischer and R. Weiss, *Acta Crystallogr., Sect. C*, 1997, **53**, 1027.
23 A. Giraudeau, H. J. Callot, J. Jordan, I. Ezhar and M. Gross, *J. Am. Chem. Soc.*, 1979, **101**, 3857.
24 S. Dahal, M. Nethaji and V. Krishnan, *Acta Crystallogr., Sect. C*, 1994, **50**, 314.
25 M. O. Senge, unpublished work.
26 H. H. Inhoffen, J.-H. Fuhrhop, H. Voigt and H. Brockmann Jr., *Liebigs Ann. Chem.*, 1966, **133**, 695; J. W. Buchler, in *The Porphyrins*, ed. D. Dolphin, Academic Press, New York, 1978, vol. 1, p. 389.
27 T. Ema, M. O. Senge, N. Y. Nelson, H. Ogoshi and K. M. Smith, *Angew. Chem., Int. Ed. Engl.*, 1994, **33**, 1879; M. O. Senge, T. Ema and K. M. Smith, *J. Chem. Soc., Chem. Commun.*, 1995, 733; W. Jentzen, M. C. Simpson, J. D. Hobbs, X. Song, T. Ema, N. Y. Nelson, C. J. Medforth, K. M. Smith, M. Veyrat, M. Mazzanti, R. Ramasseul, J.-C. Marchon, T. Takeuchi, W. A. Goddard III and J. A. Shelnutt, *J. Am. Chem. Soc.*, 1995, **117**, 11085; S. Gentemann, C. J. Medforth, T. Ema, N. Y. Nelson, K. M. Smith, J. Fajer and D. Holten, *Chem. Phys. Lett.*, 1995, **245**, 441.
28 M. Veyrat, R. Ramasseul, J.-C. Marchon, I. Turowska-Tyrk and W. R. Scheidt, *New J. Chem.*, 1995, **19**, 1199.
29 M. O. Senge, I. Bischoff, N. Y. Nelson and K. M. Smith, *J. Porphyrins Phthalocyanines*, 1998, in the press.
30 T. J. Wijesekera, J. E. Lyons and P. E. Ellis Jr., *Catal. Lett.*, 1996, **36**, 69.
31 K. M. Smith (editor), *Porphyrins and Metalloporphyrins*, Academic Press, New York, 1975.
32 H. Hope, *Prog. Inorg. Chem.*, 1994, **41**, 1.
33 S. R. Parkin, B. Moezzi and H. Hope, *J. Appl. Crystallogr.*, 1995, **28**, 53.
34 G. M. Sheldrick, SADABS, a program for absorption correction using area detector data, Universität Göttingen, 1996.
35 G. M. Sheldrick, SHELXS 97, Program for Crystal Structure Solution, Universität Göttingen, 1997.
36 G. M. Sheldrick, SHELXL 97, Program for Crystal Structure Refinement, Universität Göttingen, 1997.

Paper 8/06460A